National Défense
Defence nationale

A TEM CELL FOR ELECTROMAGNETIC PULSE APPLICATIONS: DESIGN CONSIDERATIONS AND MECHANICAL DETAILS (U)

by

J.S. Seregelyi, R. Apps and J.A. Walsh

DEFENCE RESEARCH ESTABLISHMENT OTTAWA
REPORT NO. 1263

Canada

March 1995
Ottawa

National Defence / Défense nationale

A TEM CELL FOR ELECTROMAGNETIC PULSE APPLICATIONS: DESIGN CONSIDERATIONS AND MECHANICAL DETAILS (U)

by

J.S. Seregelyi, R. Apps and J.A. Walsh
Countermeasures Section
Electronic Warfare Division

DEFENCE RESEARCH ESTABLISHMENT OTTAWA
REPORT N0. 1263

PCN
041LT

March 1995
Ottawa

ABSTRACT

This report discusses the mechanical details and some electrical properties of a Transverse Electromagnetic (TEM) cell, an Electromagnetic Pulse (EMP) generator and a terminating network. It is an implementation of a design described in detail in DREO Report No. 1084 (1991) [1]. The cell is primarily designed to generate the fast rise time (few ns) and high field levels (50 kV/m) associated with an EMP. However, it is fabricated in a modular format so that, for example, the high-voltage pulse generator can be removed and replaced with an extended taper that will allow conventional EMC measurements to be performed. Such a format significantly increases the versatility of the cell.

RÉSUMÉ

Ce rapport présente les détails mécaniques ainsi que quelque unes des propriétés électriques d'une cellule de champ électromagnétique transversal, incluant un générateur d'impulsions électromagnétique (IEM) et un réseau terminateur. Il s'agit de la réalisation du système décrit en détail dans le rapport #1084 (1991) [1]. Cette cellule a été particulièrement conçue pour permettre la génération et la propagation d'impulsions extrêmement rapides avec un temps de montée de l'ordre de quelques nanosecondes. Le champ généré est aussi très intense (50 kV/m) pour permettre de simuler adéquatement une IEM nucléaire. La cellule a été conçue de façon modulaire pour pouvoir de remplacer le générateur par une section effilée permettant d'effectuer des mesures de compatibilité électromagnétique conventionnelle, rendant cette cellule extrêmement versatile.

EXECUTIVE SUMMARY

Electromagnetic Pulse (EMP) simulators are designed to emulate the intense EMP generated by an exploding nuclear weapon and, subsequently, are used to evaluate the susceptibility of CF electronic systems against the effects of EMP. This report is concerned with the development of a small, co-axial type of EMP simulator intended for both routine testing (MIL-STD-461C) and for R&D purposes such as; calibration of sensors, precision measurements, design and testing of transient suppression devices etc.

In addition, the cell has been designed in a modular format so that it can be used for other types of measurements. For example, the high-voltage pulse generator can be removed and replaced with an extended taper for conventional EMC measurements. This significantly increases the versatility of the cell.

A discussion of the electrical design of the TEM cell was previously presented in DREO Report No. 1084. The present report is an implementation of the above work and discusses both the mechanical requirements and the resulting electrical characteristics of the constructed cell.

After assembly and testing it was concluded that the electrical parameters of the cell were accurately predicted prior to construction and achieved through careful assembly. A significant effort was made to ensure that; the cell dimensions were accurately reproduced, that the required panel joints produced negligible perturbation of the current flow, access to the test volume was user-friendly to simplify lengthy test sequences and that the design of the high-voltage pulse source and termination have been optimized. In addition, the design emphasizes the use of common construction materials and simple assembly techniques for cost reduction.

The result of the above efforts is a relatively low-cost TEM cell which produces a pulsed electromagnetic field with a peak value of 50,000 V/m with only insignificant deviations from an ideal double-exponential waveshape. The benefit of having such an accurate and highly reproducible waveform is the simplification in the interpretation of future experimental results.

TABLE OF CONTENTS

1.0 INTRODUCTION

A TEM (Transverse Electric and Magnetic) cell is a square or rectangular coaxial transmission line tapered at each end to form an enclosed unit. The cell is fed at one end with a signal generator and terminated at the other end by a resistor equal to the characteristic impedance of the line. Between the inner conductor (the septum) and the grounded metal exterior, an electromagnetic (EM) field propagates from the source to the termination in a fashion similar to planar fields in free space, see Fig. 1. The exterior of the cell also forms an enclosure which both contains the internal field (that would otherwise radiate into the surroundings and perhaps interfere with peripheral equipment) and, conversely, shields the internal volume from the external electromagnetic environment, e.g. from nearby broadcast transmitters. An additional advantage of the TEM cell is that the field is well characterized and reasonably uniform in the test volume. The primary shortcomings are an upper frequency limit determined by the size of the cell and the restricted working volume.

The source at the input side can be continuous wave (CW) from a network analyzer etc. or a pulse generator. In a conventional cell, the source and termination are connected by coaxial cables. In the case of an EMP simulator, the pulse generator and terminating resistor may be integrated into the coaxial structure of the cell to form a completely enclosed unit. This optimizes the bandwidth of the interfaces while eliminating the high voltage difficulties encountered with standard connectors. In the DREO TEM cell, the input and termination interfaces have been designed in a modular form to allow use as either a conventional cell or an EMP cell. As a result, it is possible and relatively simple to implement applications such as:

- susceptibility testing of small equipment;
- calibration of sensors;
- design and testing of countermeasures;
- and measurement of transfer functions.

In the design report [1], details for both a 50 Ω or 100 Ω TEM cell were presented. In this report the latter has been implemented for the following reasons:

- The larger impedance results in a smaller septum width. This reduces the opportunity of high voltage flash-over at the ends of the tapers where the septum/cell wall separation becomes relatively small;

- The higher impedance of the cell raises the cutoff frequency of the first non-TEM (Transverse Electric and Magnetic) mode and, thus, allows higher bandwidth testing. In addition, the higher impedance allows easier coupling of the high frequencies of the pulse generator to the cell and, therefore, allows faster rise time pulses to be produced;

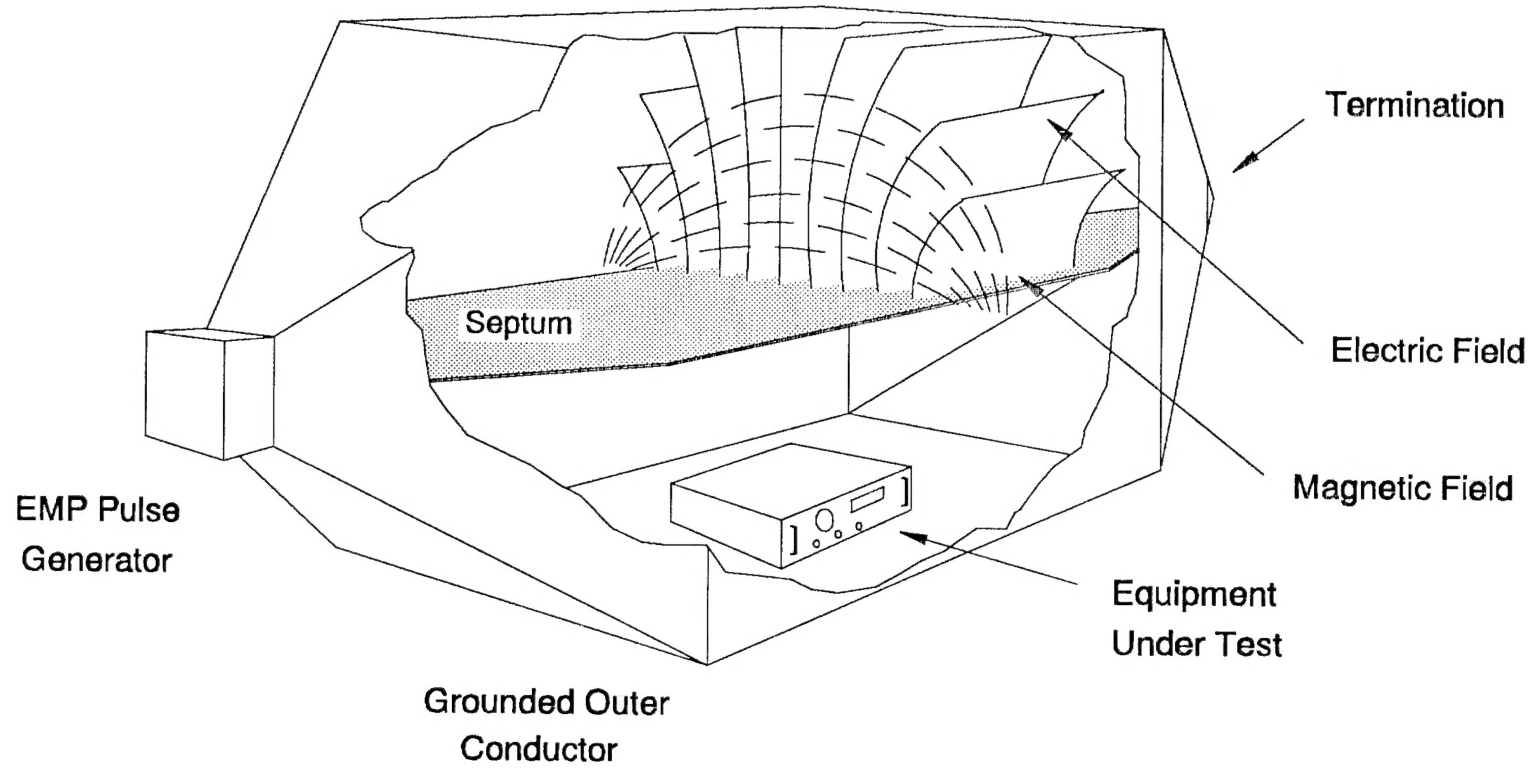

Figure 1: Schematic representation of the TEM cell. The flat central portion of the transmission line is truncated by tapered ends. One end contains a pulse generator or CW source and the other is terminated with the cell's characteristic impedance. Any test object which is placed in the bottom of the cell will be subjected to the electric field formed by the voltage difference between the septum (inner conductor) and the grounded outer conductor.

- The 100 Ω impedance is compatible with the power amplifier presently available in the lab. This amplifier, when driven by an AM/FM signal generator or the arbitrary waveform generator will allow a multitude of lower voltage tests (<1500 V/m) to be performed;

- Compatibility with the requirements of MIL-STD-461C.

The main disadvantages of having chosen the 100 Ω impedance is that it is more difficult to make use of standard 50 Ω equipment and the field uniformity is marginally poorer.

2.0 TEM CELL MECHANICAL DETAILS

A test volume height of 30 cm was deemed adequate for the cell since most DUT (device under test) are of this size or smaller. This dictates that the septum height be at least 3 x 0.3 m so that the field disturbance produced by the DUT is tolerable. The final design incorporates a septum height of 1 m which results in a structure with a 2 m square cross-section. A square cross-section is considered the optimal geometry for simultaneous maximization of test area and cell bandwidth. As a result of the above choices, the septum must have a width of 80 cm to produce the required 100 Ω impedance [8].

Since standard commercial sheet metals are available in 4' by 8' sheets, it is clear that the unit must be produced out of several panels. The 3 sections (two tapered and one central section) were each made of 8 panels for a total of 24. An overview of the cell is presented in Figs. 2-5. In addition to displaying the overall shape and size of the outer conductor and septum, these figures also shows the panel layout and hatch locations.

A length of 2 m was chosen for both the uniform cross-section and the tapers. Therefore, the total length along the center line of the cell is 6 m. The length of the tapers is relatively large for a typical TEM cell, however this results in a shorter rise time with reduced field distortion caused by reflections at the taper interfaces. The taper lengths may be made longer, the size of the room in which the cell is to be located was the limiting factor.

Note that the cell tapers are truncated 30 cm from the apex. This allows the ends of the tapers to be completed by any means necessary to integrate the source and termination of interest. This modular design is carried through to the measurement ports of the cell by the addition of hatches at the top and bottom of the cell. These are fitted with bulkhead plates to allow easy interchange of field sensors or to provide an access port for cables, monitors etc. for a DUT. The addition of the above modifications makes the cell versatile, with applications ranging from low-voltage CW to high-voltage pulse work.

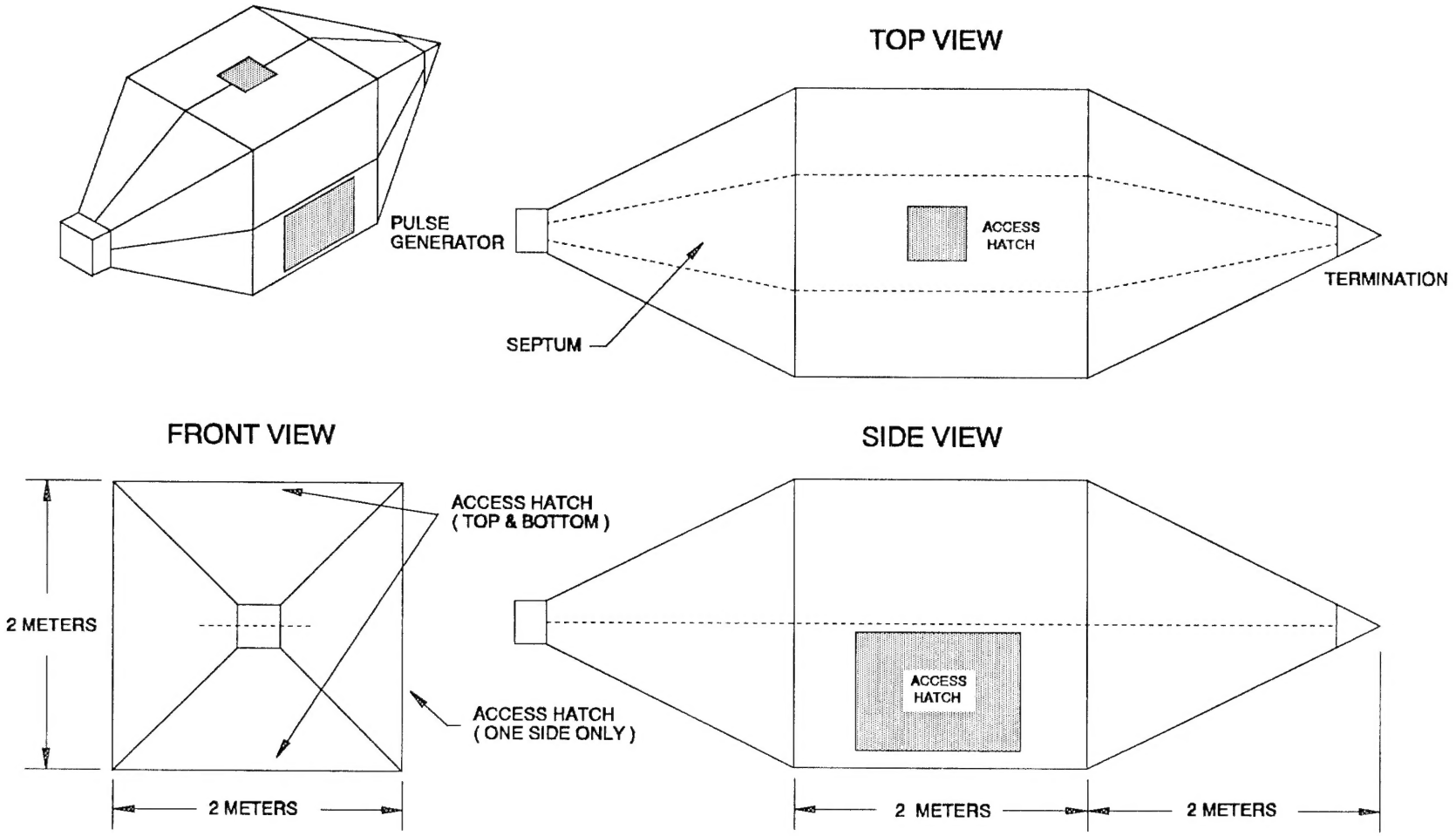

Figure 2: Overview of the TEM cell. There are two small access hatches on the top and bottom of the cell for sensors and cables, respectively. A large access is provided on one side to place test objects inside the cell. The three-dimensional image gives an indication of the panel layout of the cell.

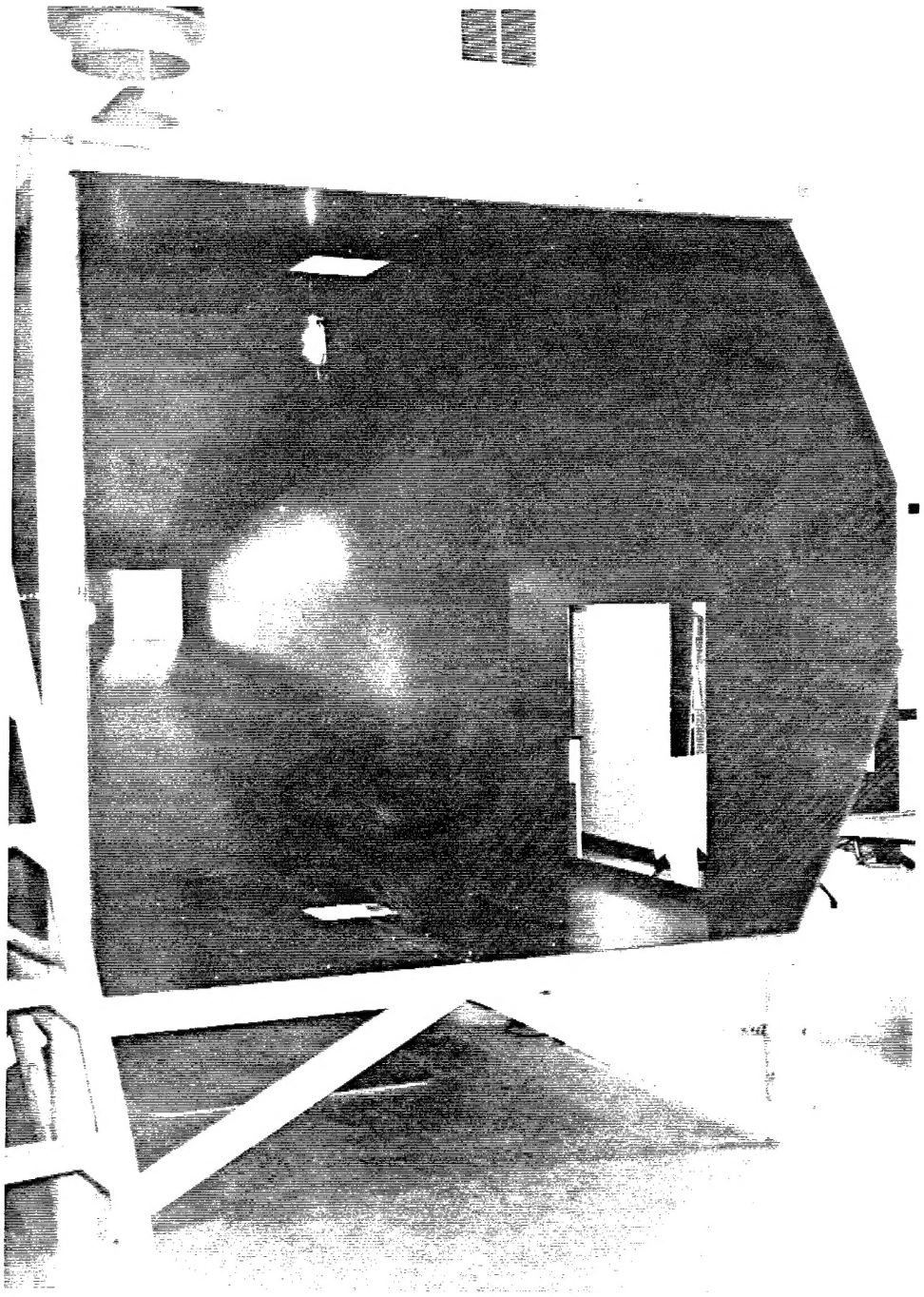

Figure 3: A view of the interior of the cell during construction. The access hatches can clearly be seen. Note that the tapers are truncated 30 cm from the end to form the interface for the removable pulse generator and termination.

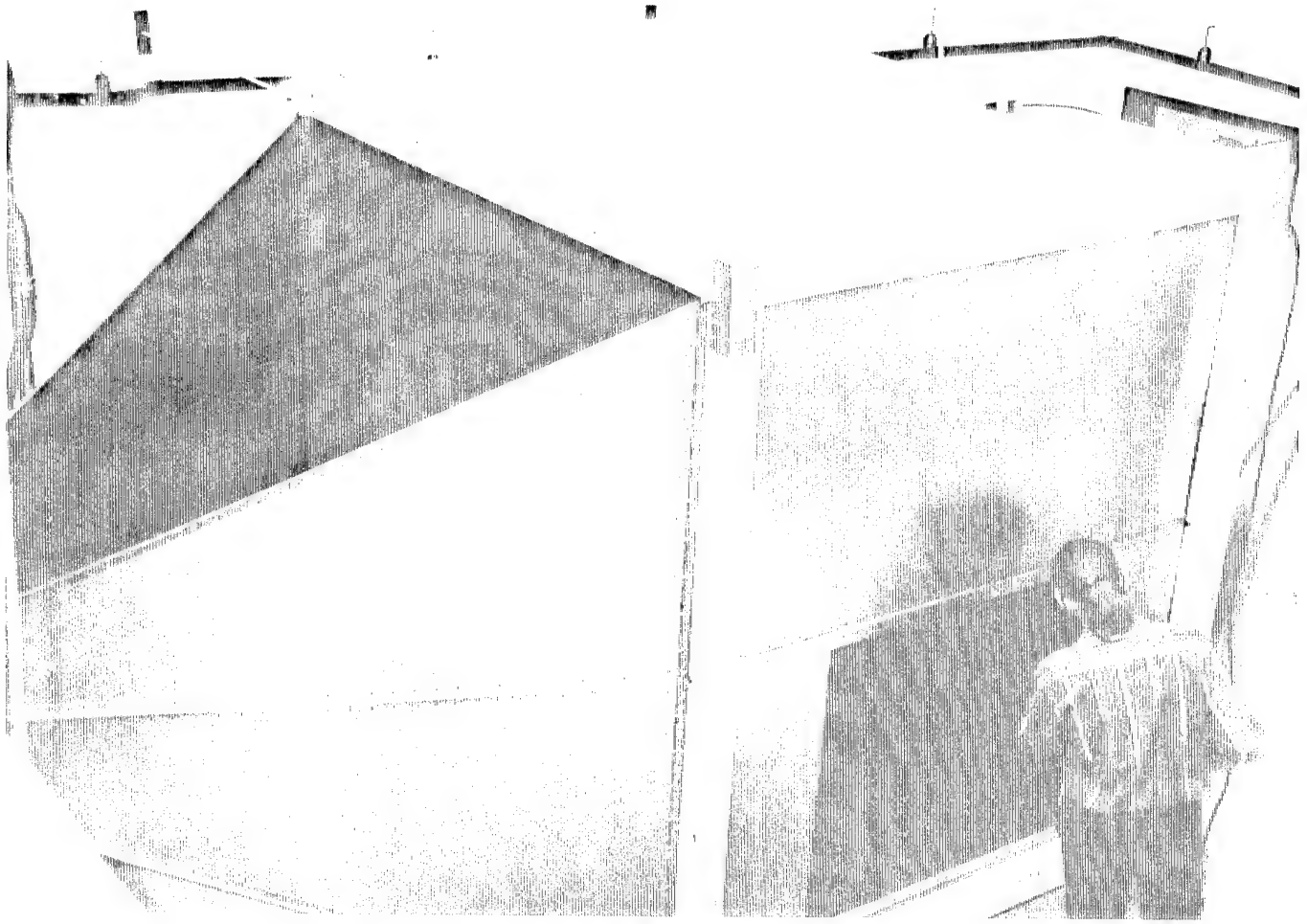

Figure 4: An additional construction photo showing the various panels which form the cell and the wooden support structure.

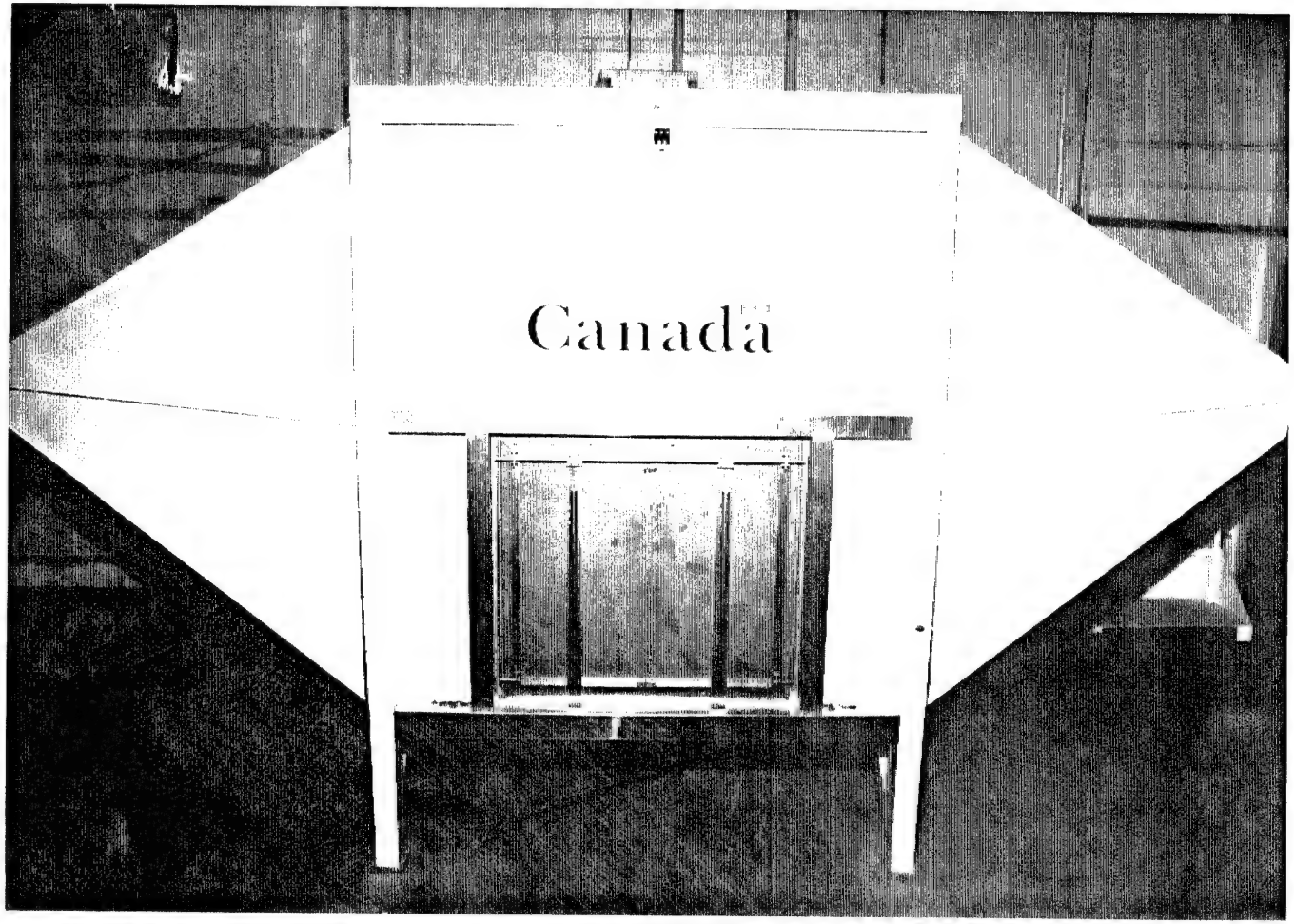

Figure 5: An overview of the completed cell.

2.1 Panel Details

As indicated above, the cell was constructed out of a series of panels. The detailed size and shape of each panel is indicated in Figs. 6-9. As can be seen, the triangular sections were designed such that two sections could be cut from one 20 gauge, 4' by 8' sheet (thereby minimizing waste). These two panels then formed one side of the taper. This process was repeated for each side of the front and back taper. The panels were joined by screwing together the flanges which are spot-welded to their edges, see Fig. 10 for details. Using this technique, a virtually seamless joint could be manufactured. The seam discontinuities were further reduced by covering each joint with a layer of copper tape (with conductive adhesive).

2.2 Hatch Details

2.2.1 Main Access Hatch

In order to provide access to the test volume inside the cell, some type of hatch is required. The difficulty is that this door must not disturb the continuity of the current in the cell (so as to minimize the field perturbations) while simultaneously allowing the user to easily access the DUT. The solution to this problem is shown in Figs. 11 & 12. The flange/finger-stock combination provides ample shielding and cell wall continuity while allowing simple push on/pull off operation of the door. The guide track shown in Fig. 11 is a means of ensuring proper alignment of the door during closure, while providing an out-of-the-way storage location when the cell is open. The finger stock is contained in a housing on the door so as to minimize the opportunity for damage. The unit can be disassembled for maintenance.

2.2.2 Generator Access Hatch

Access to the pulse generator is occasionally required for operational adjustments. However, it is critical that there be cell wall continuity in this area since it is both the launching point for the electromagnetic wave and the portion of the cell which must endure the highest field strengths (for much longer time periods than the EMP because of charging times, firing delays etc.). A mechanism similar to that used in the hatch above was incorporated at this point. As in the main hatch, a piece of sheet metal was shaped to fit into the hole cut in the generator wall. This was then placed on the surface of the hatch door such that when it was in place the inner wall of the generator was smooth and flush with only a small seam at the edges.

2.2.3 Sensor/Bulkhead Hatch

In order to provide access for field sensors inside the test volume or to allow control or monitoring cables to access a test object, an access port is required near the center of the test volume. In this DREO cell, a 25 cm square port was placed both at the

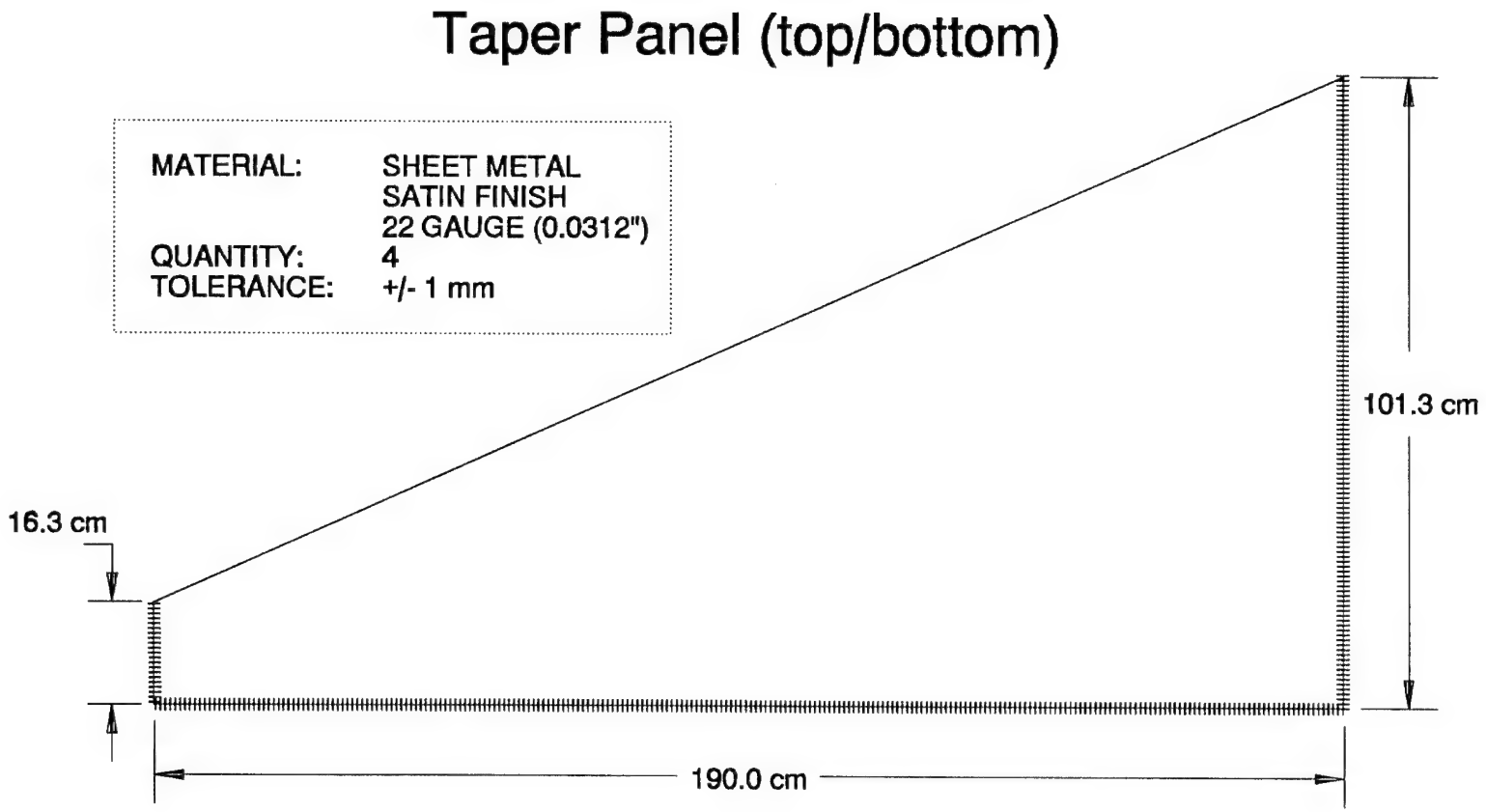

Figure 6: Detail of the panel located at the top and bottom of the cell tapers. The cross-hatched edges represent the edges that are mounted with a flange lip as described in Fig. 10. The remaining edges act as a receptacle for a flange from another panel.

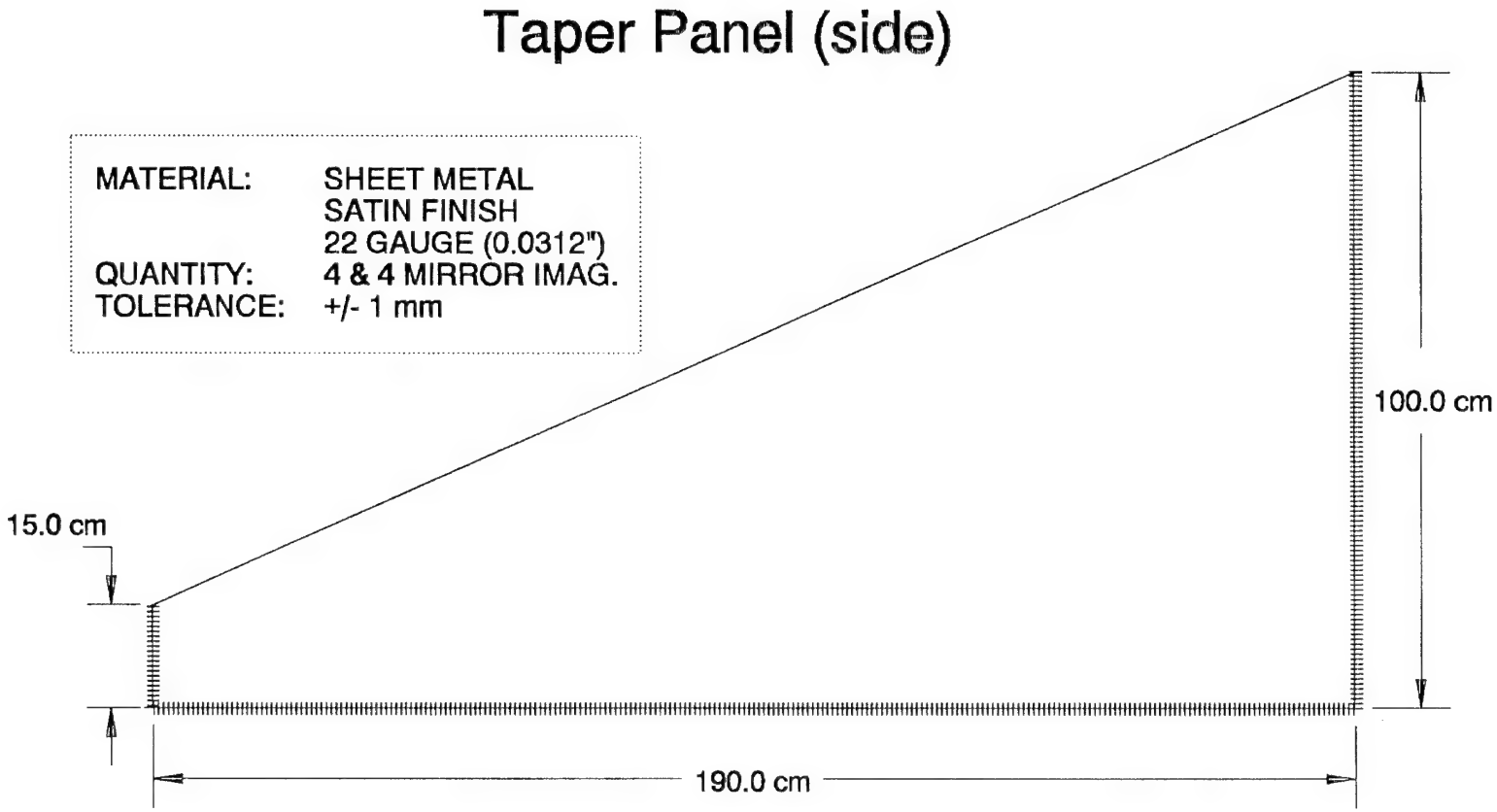

Figure 7: Detail of the panel located at the sides of the cell tapers. The cross-hatched edges represent the edges that are mounted with a flange lip as described in Fig. 10. The remaining edges act as a receptacle for a flange from another panel.

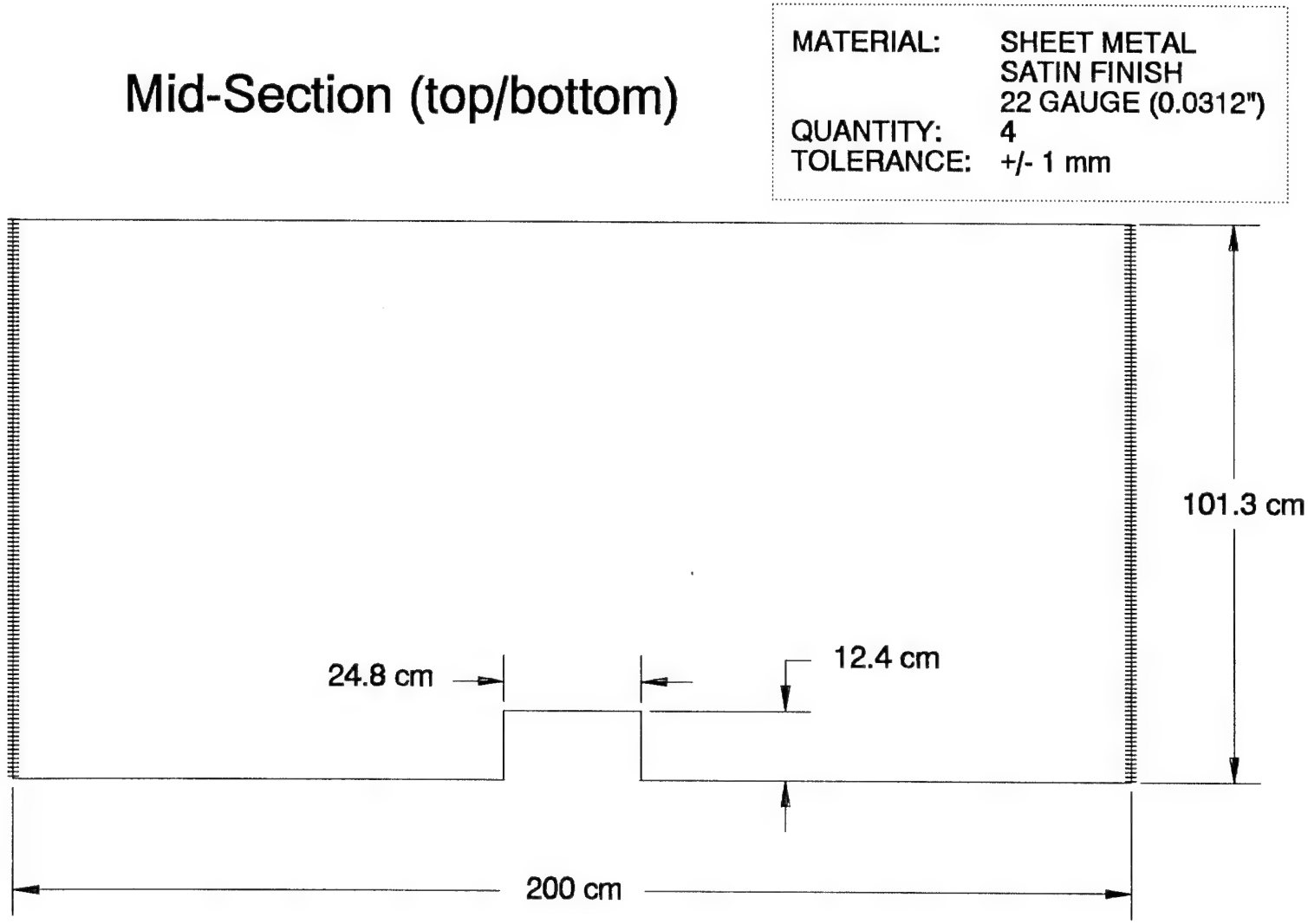

Figure 8: Detail of the panel located at the top and bottom of the central portion of the cell. The cross-hatched edges represent the edges that are mounted with a flange lip as described in Fig. 10. The remaining edges act as a receptacle for a flange from another panel.

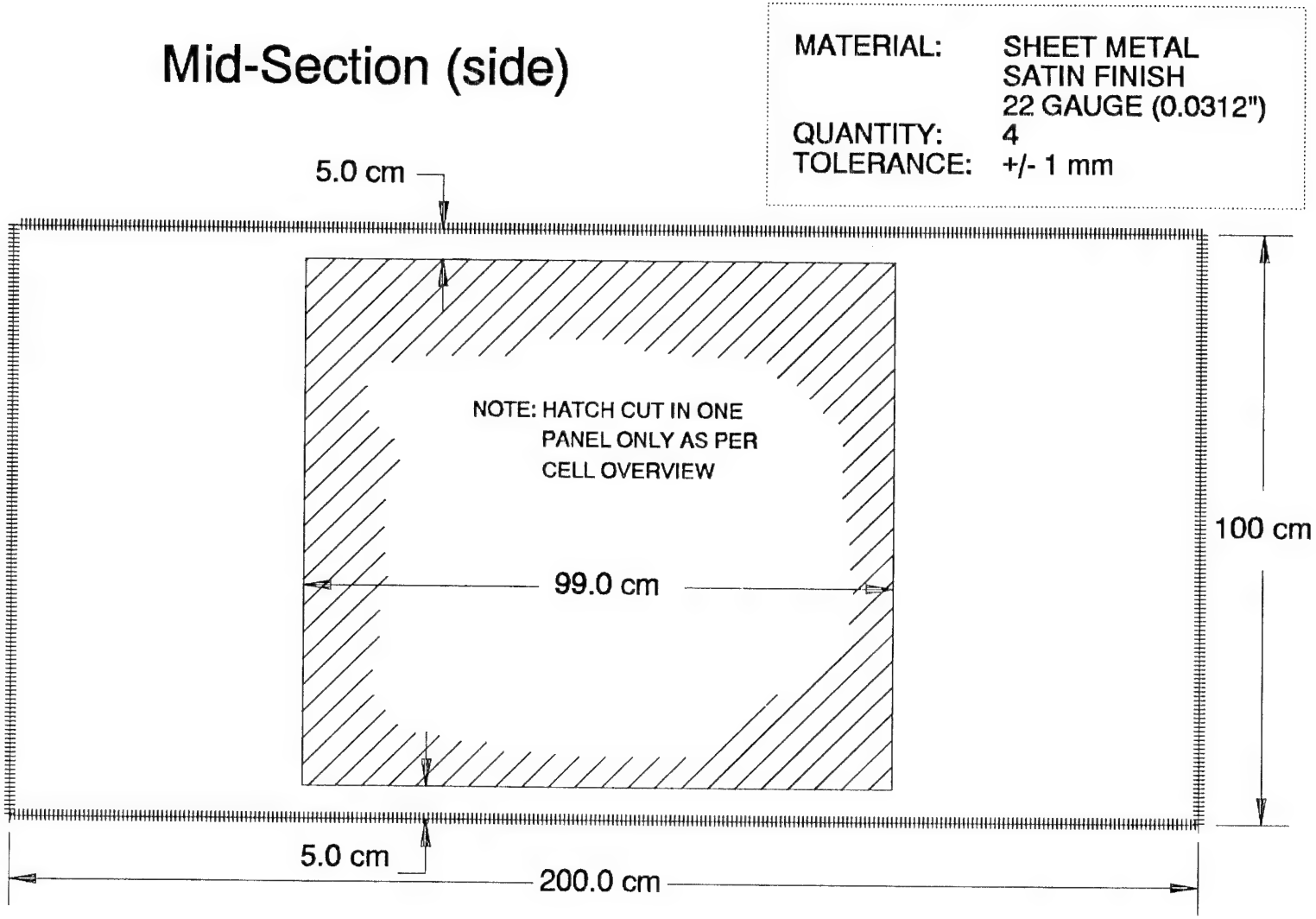

Figure 9: Detail of the panel located at the sides of the central portion of the cell. The cross-hatched edges represent the edges that are mounted with a flange lip as described in Fig. 10. The remaining edges act as a receptacle for a flange from another panel.

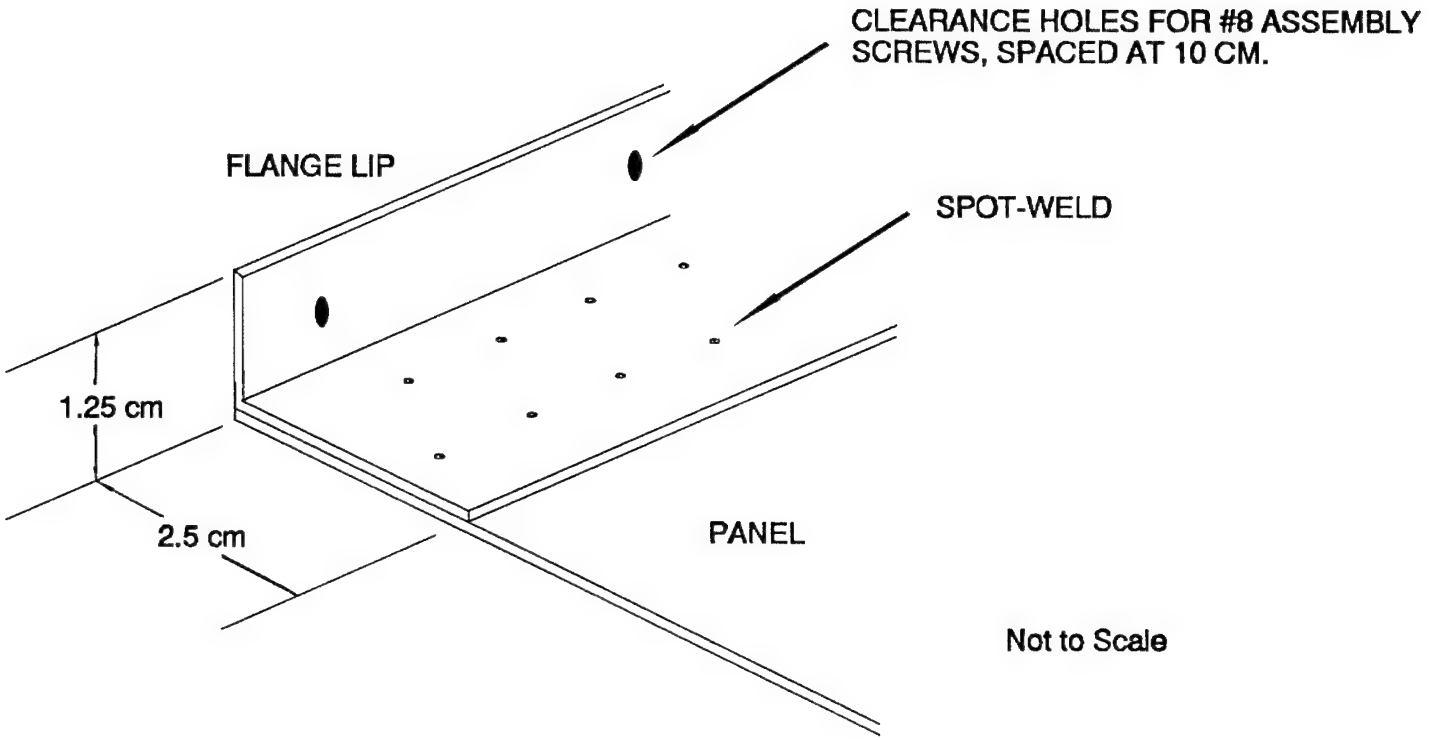

Figure 10: Detail of the flange lip on the panels in Figs 6-9. The base is spot welded to the panel while the lip provides a series of clearance holes for the alignment screws. The flange also becomes a structural support for the panel.

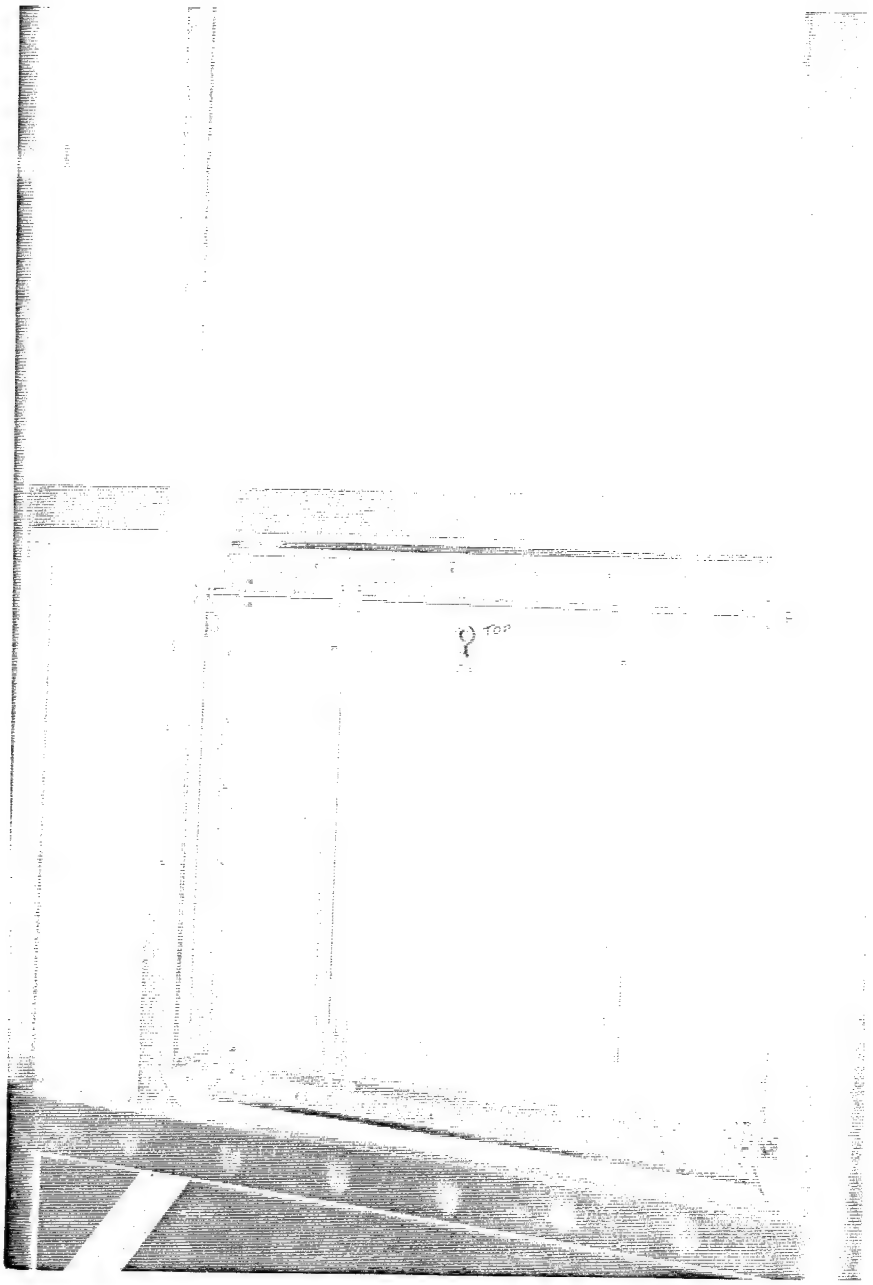

Figure 11: Photo of the side access door and assembly. The door is pulled out approx. 10 cm and is then raised in the guide track (a counter weight can be attached to the door to facilitate this process). Contact to the cell is made via the finger stock arrangement detailed in Fig. 12.

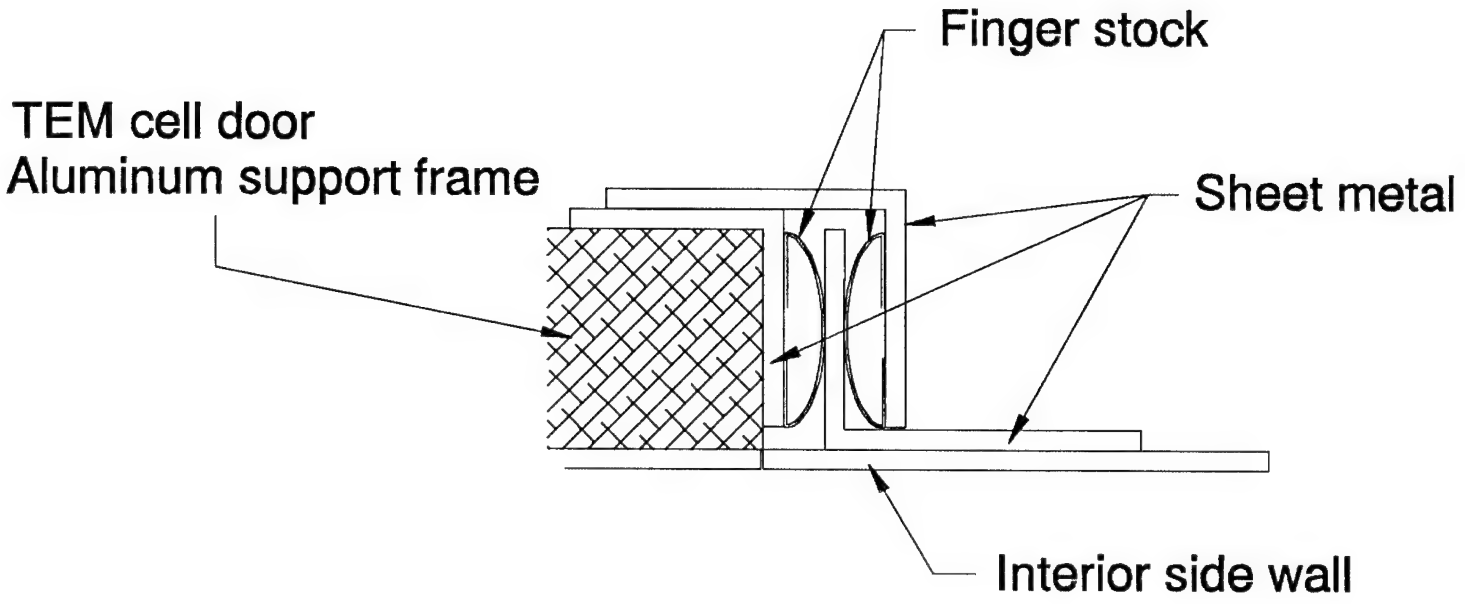

Figure 12: Detail of the finger stock mechanism which runs around the perimeter of the side access hatch. The double row of finger stock will provide ample contact while making the interior of the cell easily accessible. The mechanism can be disassembled for cleaning.

top and bottom of the central portion of the cell as indicated in Figs. 2 & 8. Details of these hatches assemblies are available in Fig. 13. The top access is intended primarily as a sensor mount, while the bottom is intended for general use. Unlike the previous case, flat finger stock was used on this hatch. This was done so that the bulkhead plate would sit reasonably flush against the bottom of the cell.

2.3 Septum and Septum Support Structure

The septum is the central portion of the co-axial TEM cell. In the DREO cell it is made of a single aluminum sheet (chosen to reduce the weight of the unit) cut as per Figs. 14-16. The latter figure details the end cuts which interface with the pulse generator and termination. The septum must be accurately supported in the cell at a height of 1 m. In addition, it is preferred that no metal and as little dielectric material as possible be present to do this. The above was accomplished by creating a support structure out of commercial fishing line. By spacing a fishing-line truss (see Fig. 17) every 50 cm along the septum, the structure is easily supported by a negligible amount of dielectric. To eliminate the small amount of buckling that does occur, a 7.5 cm rigid styrofoam sheet (Dow HI-100, dielectric const. of approx. 1.095) was ripped on a table saw to a 10 cm width. Along the center of this strip a 2.5 cm deep groove was cut. This was then pressed onto the edge of the septum to force it flat. Using this technique, a very accurate positioning of the septum was possible.

2.4 Wooden Support Structure

The sheet metal used to construct the cell is self-supporting, however, to raise the cell off the floor (to provide access to the bottom hatch) and to allow an operator to climb on top of the cell (to provide access to the top hatch) a wooden support structure has been incorporated into the design. The basic layout is shown in Figs. 4, 18-20. The unit is composed of a top and bottom panel each of which is supported by side posts. The panels were designed with basic housing construction in mind (Figs. 19 & 20). Note that the central portions have been left open so that the sensor hatches on the cell can be accessed. In addition, a series of 10 cm holes have been cut in the panels to allow for future sensor locations etc. One modification that would be made is to replace each 4x4 side support with two bonded 2x4's. This would eliminate splitting and warping of the column.

An addition support for the wooden structure was constructed by mounting a set of ½" threaded rods to the wall immediately beside the cell and connected these to the cell via a bracket (see Fig. 4, upper left corner). Once the (metal) central portion of the TEM cell had been installed inside the wooden support, these brackets were gradually adjusted (by rotating the locking nuts) to square the TEM cell precisely and lock it in place.

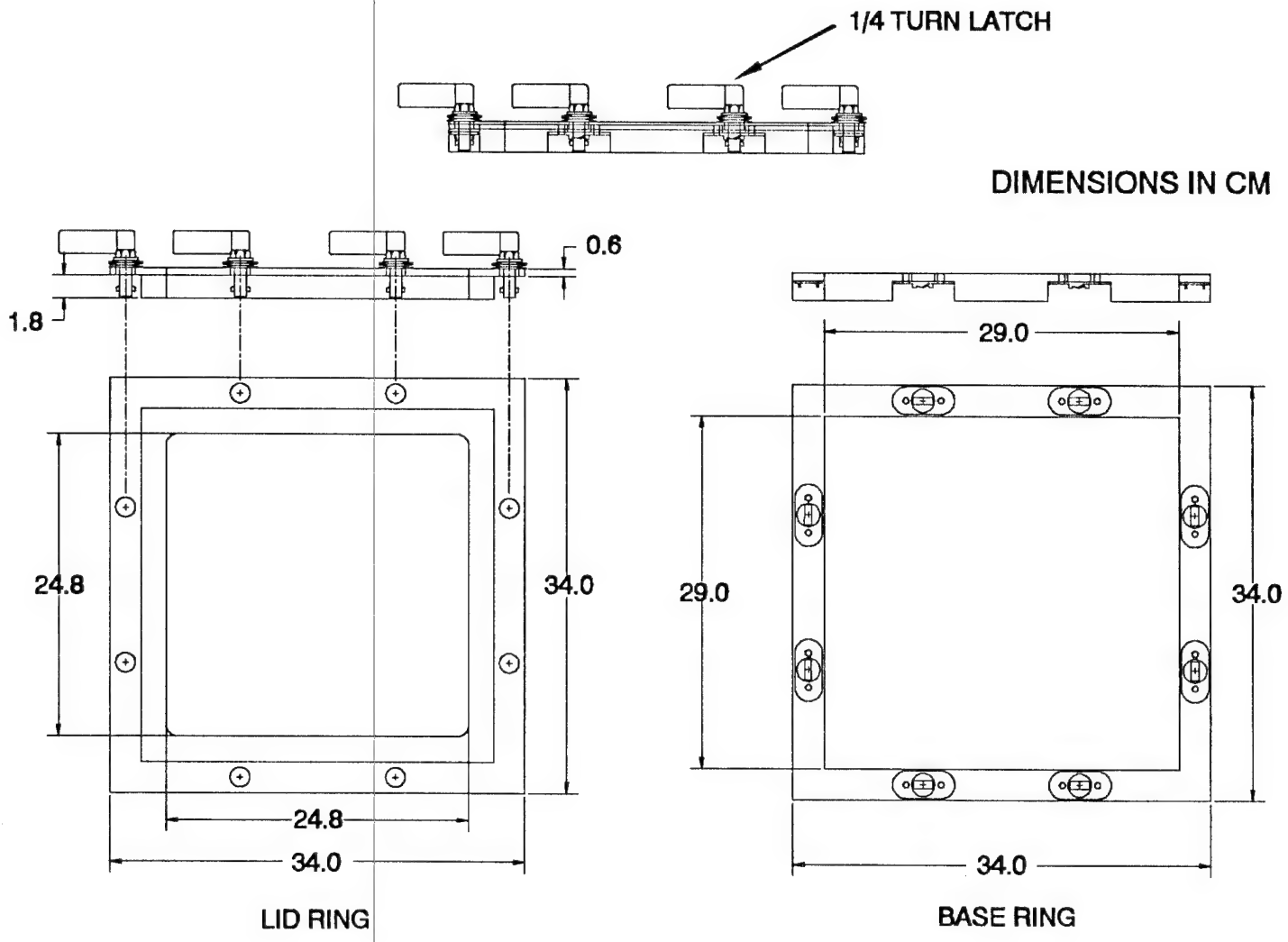

Figure 13: Detail of the access hatch assembly used on the top and bottom of the cell. The base ring is bonded directly to the TEM cell while the lid is removable (1/4 turn latch). Between the base and the lid is sandwiched a 3mm brass plate on which sensors or various connectors can be mounted. The plate is a simple 27 cm square which can be easily manufactured and replaced. It maintains contact with the cell via flat finger stock.

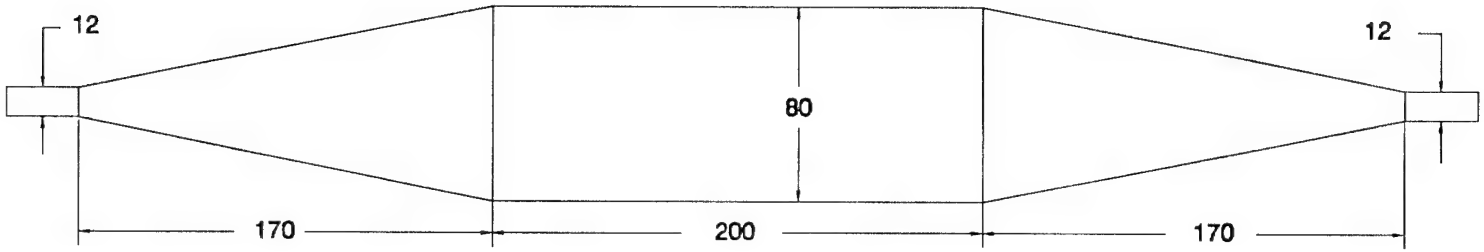

TEM Cell Septum (center conductor)

Material: Aluminum sheet (0.159 thick)
Quantity: one
Dimensions in cm

Figure 14: TEM cell septum (inner conductor). Aluminum was chosen to reduce the weight and simplify the suspension of the unit. The details of the end sections are presented in Figs. 15 and 16.

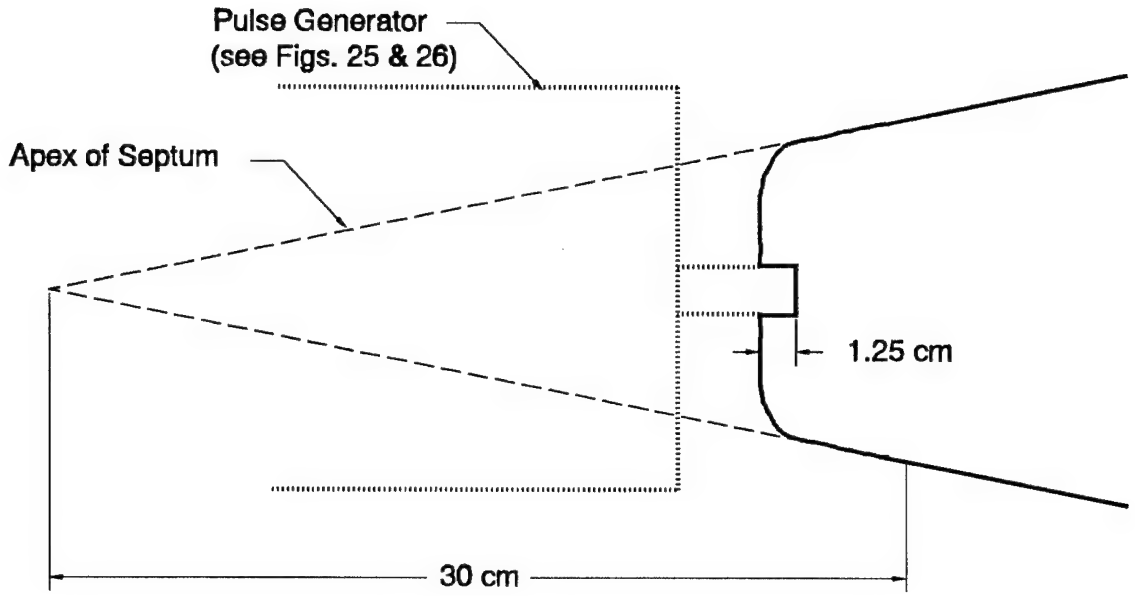

Figure 15: Detail of the source end of the septum. The dashed line represents the spark gap and capacitors of the pulse generator (Fig. 22).

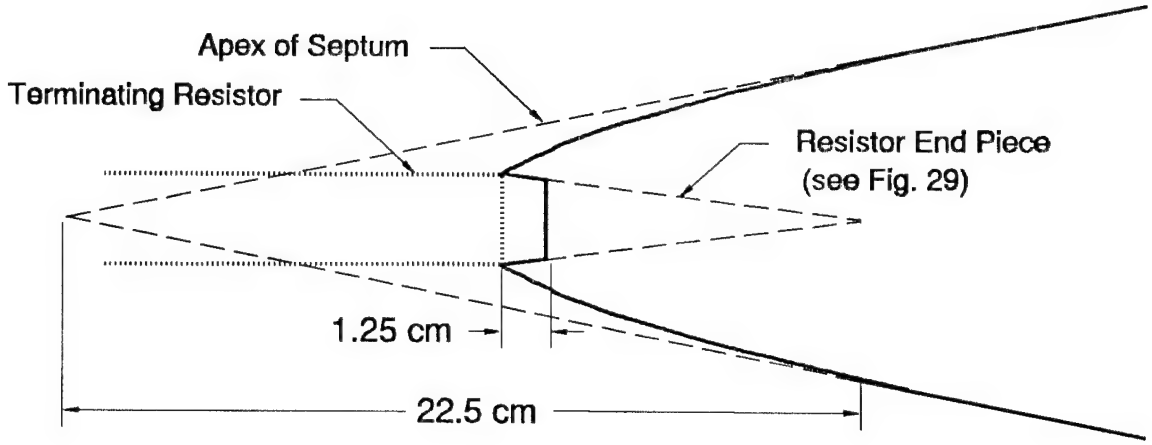

Figure 16: Detail of the termination end of the septum. The dashed line represents the high voltage resistor and the resistor end piece (Fig. 28).

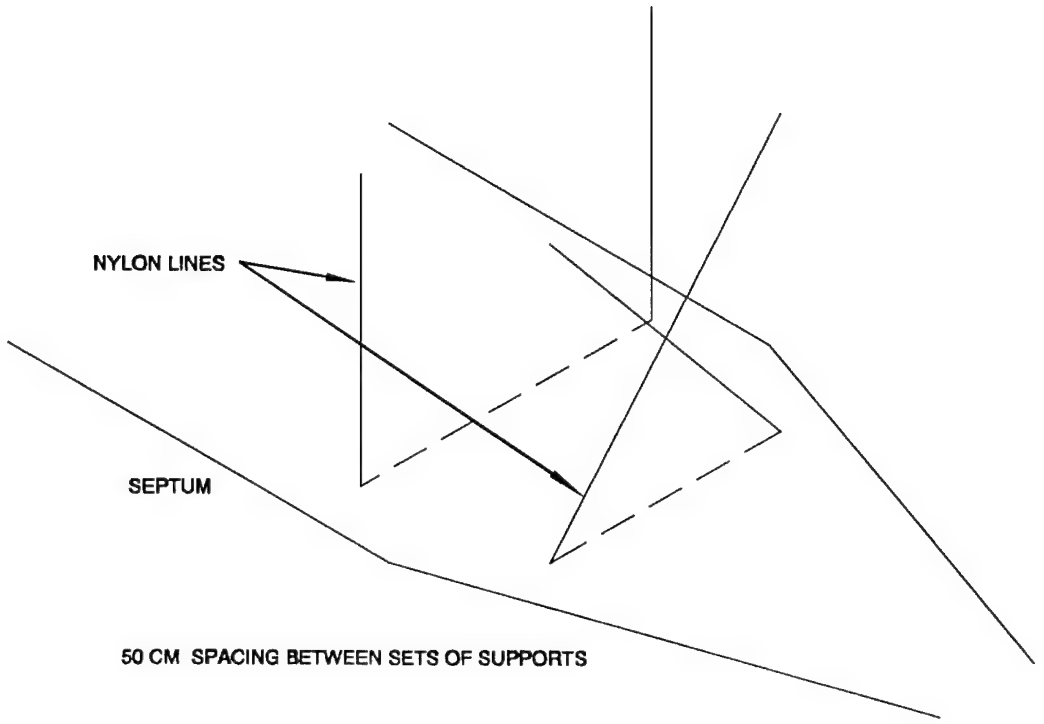

Figure 17: A series of nylon lines was used to suspend the septum. In the central area of the cell these lines are vertical and attached to the wooden support structure. This allows an operator to walk along the side of the septum. In the taper they are crossed (to minimize the swing of the septum) and suspended from the edges of the top panels (to reduce the sag in the middle of the taper).

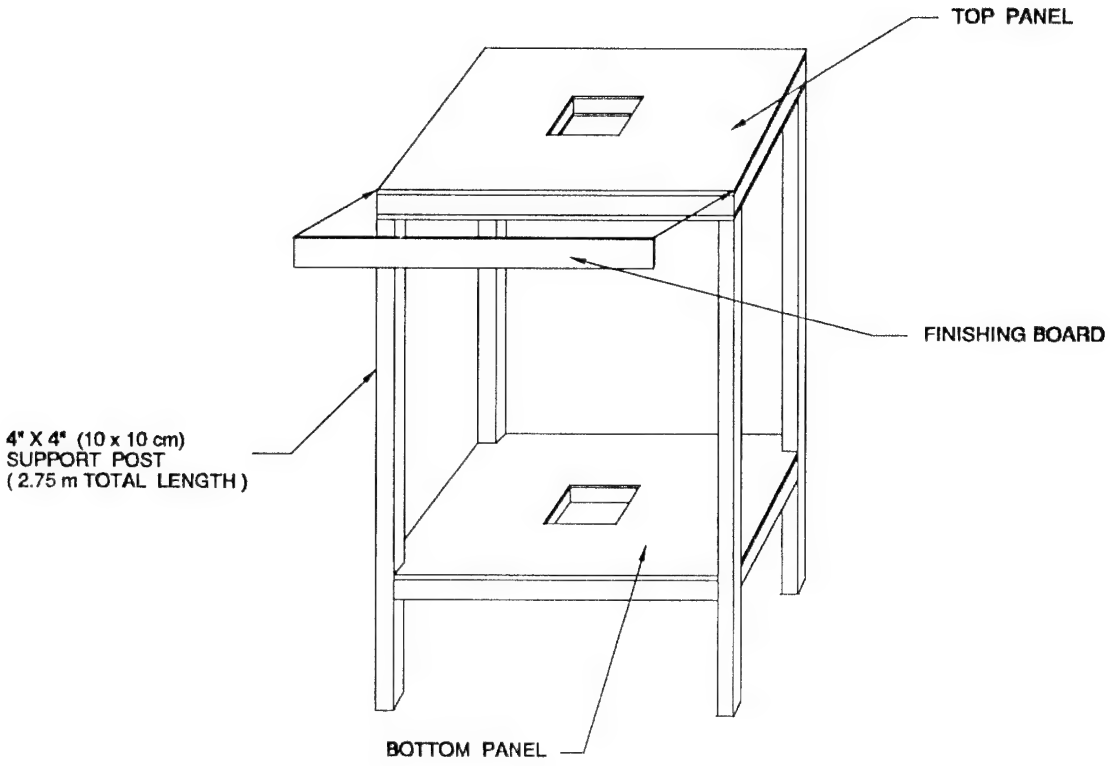

Figure 18: Overview of the TEM cell wooden support structure. Photos are provided in Figs. 3-5.

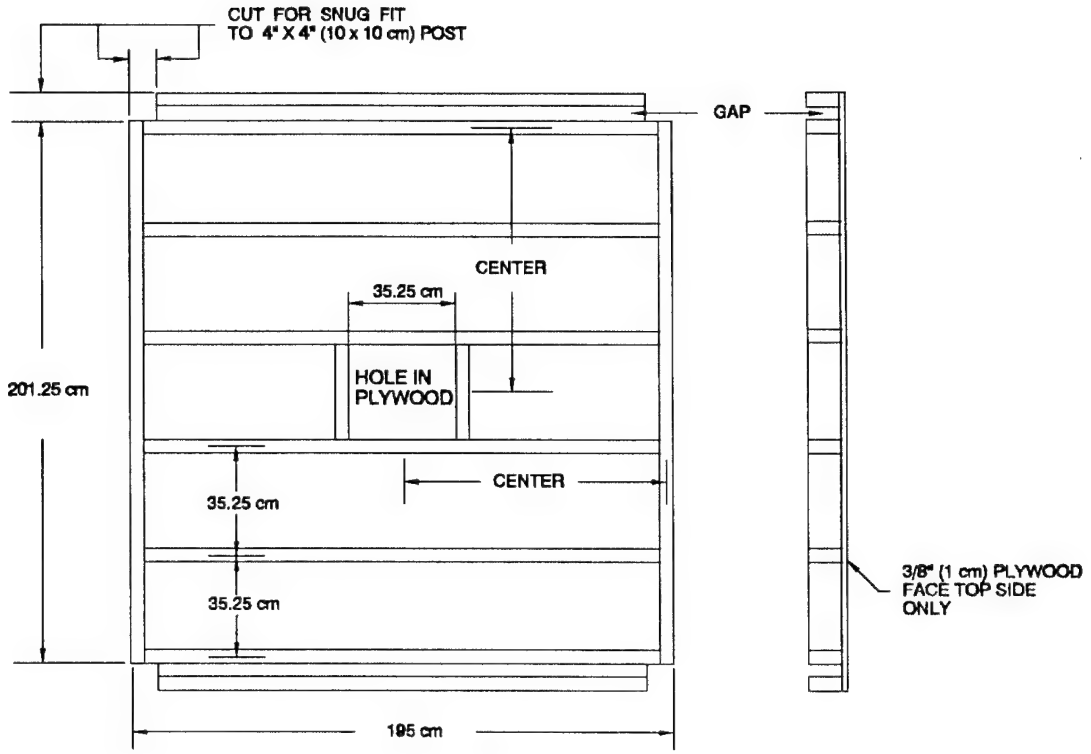

Figure 19: Detail of the bottom panel of TEM Cell wooden support structure (interior view).

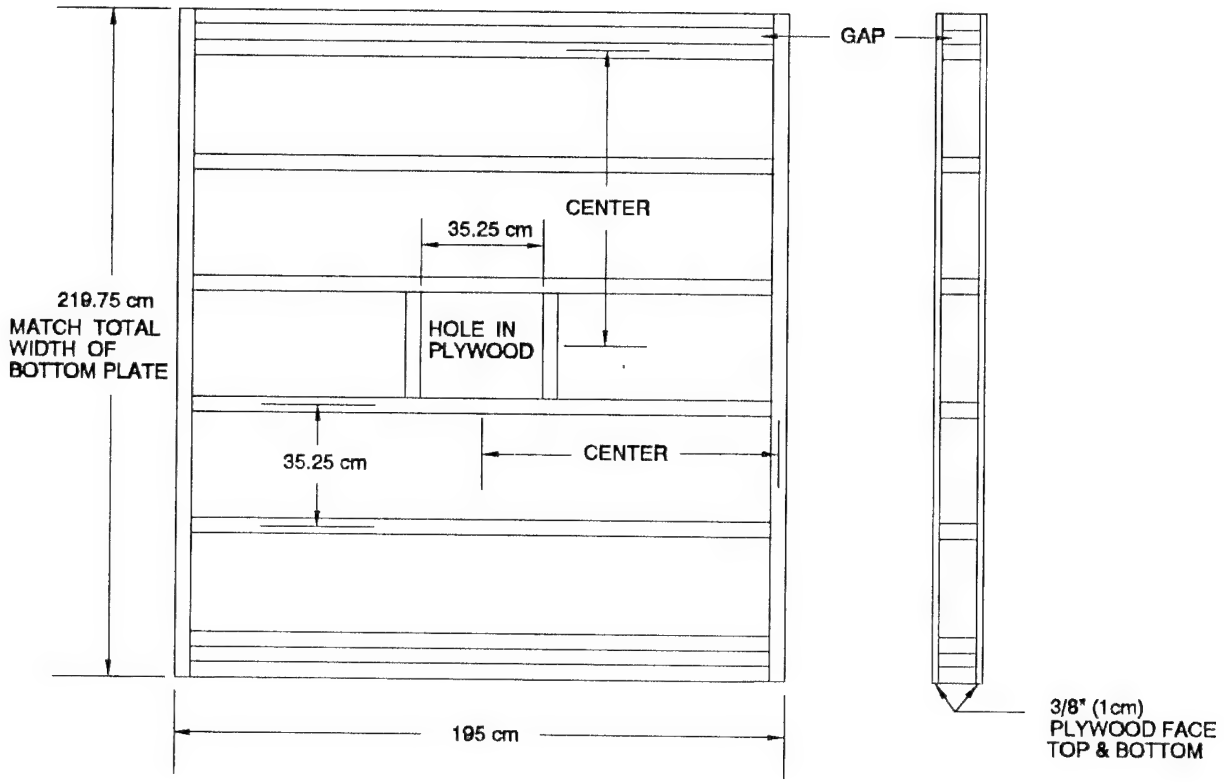

Figure 20: Detail of the top Plate of TEM Cell wooden support (interior view).

3.0 TEM CELL ELECTRICAL DETAILS

The details in this section are a summary of the main parts of Reference [1] and are reproduced here for the convenience of the reader.

3.1 Cell Impedance

The characteristic impedance of a TEM cell can be expressed as

$$Z_0 = \frac{\eta_0 \epsilon_0}{C_0} \quad \text{ohm} \tag{1}$$

where $\eta_0 = 120\ \pi$ ohm, and

$$\frac{C_0}{\epsilon_0} \approx 4\left[\frac{a}{b} - \frac{2}{\pi} \ln\left(\sinh\frac{\pi g}{2b}\right)\right] - \frac{\Delta C}{\epsilon_0} \tag{2}$$

The term $\Delta C/\epsilon_0$ relates to the fringe capacitance between the edges of the septum and the side walls and a, b and g are the dimensions of the cell, see Fig. 21. Since the dimensions a = b = 1 m were determined by the minimum test-object size and a 100 Ω cell impedance is required, then the width of the septum becomes 80 cm [8].

3.2 Frequency Domain Response

3.2.1 Transverse Electric (TE) and Magnetic (TM) Modes

TEM (Transverse Electromagnetic) waves are characterized by the fact that both the electric vector (E-field) and the magnetic vector (H-field) are perpendicular to each other and to the direction of propagation, see Fig. 1. However, a TEM cell will not only propagate a single TEM mode at all frequencies, but also a set of Transverse Electric and Transverse Magnetic higher-order modes, TE_{mn} and TM_{mn}, at frequencies above their respective cutoff frequencies $f_{c(mn)}$ [3, 4]. The TEM mode propagates through the tapered ends of the cell. Each higher-order mode, however, is always reflected at some point within the taper where the dimensions become too small for propagation. This is the point where the cross-section of the taper has narrowed to that of a waveguide whose cutoff frequency is lower than the field frequency. The propagating energy in the higher-order mode undergoes multiple reflections, end to end, within the cell, until it is dissipated.

At certain frequencies a resonance condition is satisfied, in which the cell's effective length for the mode is "p" half guide wavelengths long (p = 1, 2, ...). At these resonant frequencies $f_{R(mnp)}$, a TE_{mnp} resonant field pattern exists. Thus the TE_{mn} mode in a given TEM cell has one cutoff frequency $f_{c(mn)}$ and an infinite set of resonant frequencies, $f_{R(mnp)}$ with p = 1, 2, ... The same is true for the TM_{mn} higher-order modes.

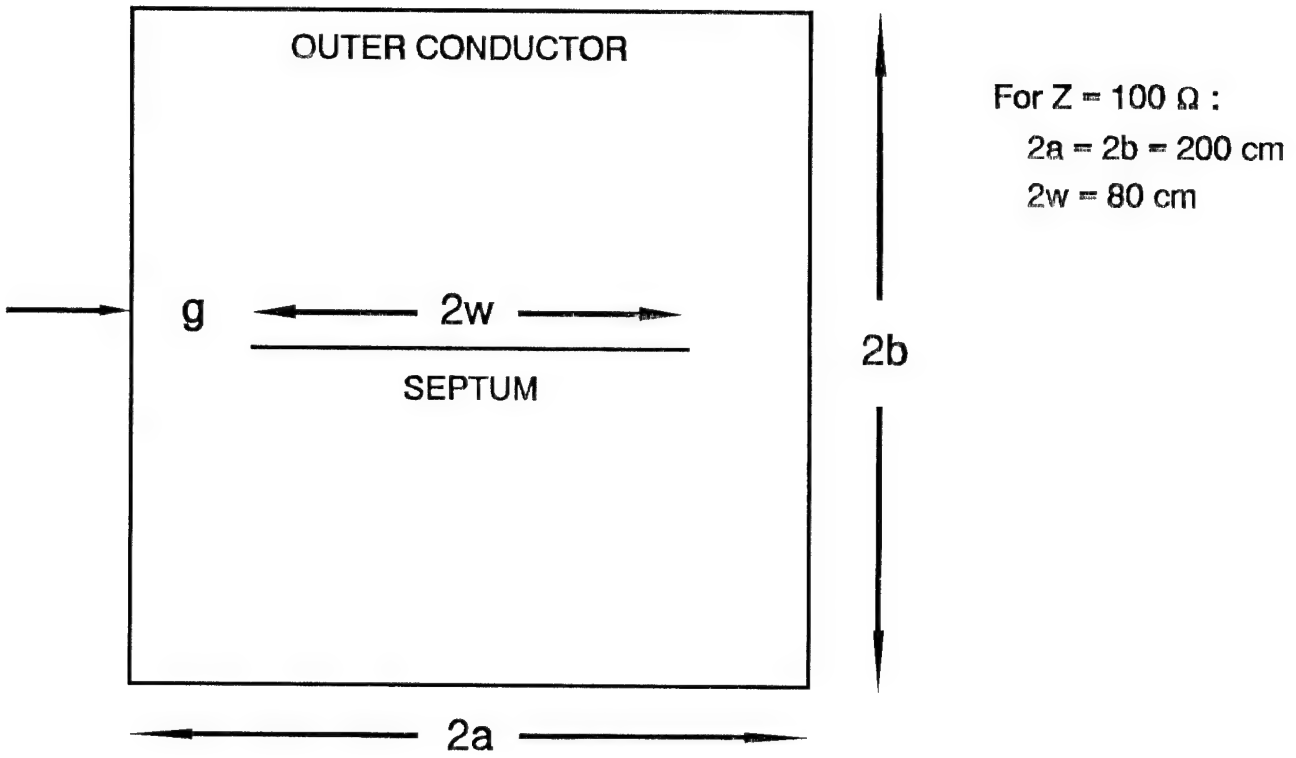

Figure 21: Definition of parameters used in the calculations

The total E-field pattern is the superposition of the fields inherent to the TEM and TE_{nmp} modes and the total H-field pattern is the superposition of the fields inherent to the TEM and TM_{nmp} modes.

The resonant frequencies, $f_{R(mnp)}$ are calculated from the values of $f_{c(mn)}$ and the cell's length and taper dimensions [1]

$$f_{R(mnp)}^2 = f_{c(mn)}^2 + \left(\frac{pc}{2L_{mn}}\right)^2 \qquad (3)$$

$$L_{mn} = L_C + X_{mn}L_E \, . \qquad (4)$$

L_C (=2 m) is the length of the uniform-cross-section central part of the cell, L_E (=4 m) is the length (along the center line) of the two tapered ends, and X_{mn} is the fraction of the two ends included in the value of L_{mn}, (fraction X_{mn} is empirically determined and is different for each cell as well as each mode. It can vary from 0.8 for the TE_{01} mode to 0.5 for the TE_{10} and TE_{11} modes).

To design a TEM cell with maximum usable bandwidth, the frequency of the first interacting resonance TE_{101} should be as high as possible. This is accomplished primarily by making cell dimension "a" as small as possible, which causes $f_{c(10)}$ to be as large as possible. The important point to note is that the frequencies depend purely on the cell geometry (dimensions a, b and w for f_c; and a, b, w and L_{mn} for f_R).

When measuring the frequency domain response of a TEM cell it is critical to keep in mind that the response at the input port of the cell can be very different from the response at some other portion of the cell. This is because the measurement is generally made with a network analyzer or some other CW source applied for a period of time such that the EM fields can traverse the length of the cell hundreds of times over. These multiple reflections can interfere both constructively and destructively to create peaks and nulls in the field response. If a field sensor were placed in a null it obviously would indicate that no field was present. This could be in contradiction with a measurement made at the input port (which is at a different location and may not be in a null). In general, it is common to overestimate the bandwidth of a TEM cell if only the response at an input port is measured.

3.3 Time-Domain Response

3.3.1 Pulse Rise Time Degradation

Since the distance from the apex to the end of the front taper along the outer conductor of the TEM cell is greater than that along the septum, it will take longer for

take longer for current to travel along the outer conductor. As a result, there will be a curvature to the wave front in the working volume of the cell. If an object is placed at this point, then the top of the object will be illuminated before the bottom. The net result will appear as a degradation in the rise time of the input pulse and is considered to be the inherent rise time of the cell.

The worst case change in rise time can be calculated from the difference in path length in the tapers. The length x, from the apex to one of the corners of the front taper.

$$x = \sqrt{L_E^2 + a^2 + b^2} \quad . \tag{5}$$

With $\frac{1}{2}L_E = 2a = 2b = 2.0$ m, this length is $x = 2.45$ m. The difference in path length between the shortest and longest path is

$$\Delta\ell = x - L_E = 0.45 \text{ m} \tag{6}$$

If current is flowing at the speed of light, then the response time associated with $\Delta\ell$ (i.e. the rise time of the cell) is

$$t_r = \Delta\ell/c = 1.5 \text{ ns} \quad . \tag{7}$$

This represents the largest possible delay in the cell. A more realistic estimate is made by looking at the path difference at the edges of the recommended test volume

$$x = \left[L_E^2 + \left(\frac{2b}{3}\right)^2 + \left(\frac{w}{6}\right)^2 \right]^{\frac{1}{2}} = 2.123 \text{ m} \tag{8}$$

$$\Delta\ell = 2.123 - 2 = 0.123 \text{ m}$$

$$t_r = \frac{\Delta\ell}{c} = 0.38 \text{ ns} \quad . \tag{9}$$

The rise time measured in the cell is related to the input pulse and the TEM cell by the relationship

$$t_{measured} = \sqrt{t_{input}^2 + t_r^2} \quad . \tag{10}$$

Although (10) is strictly true only for gaussian and exponential pulses [11], it does provide

a reasonable estimate of the field rise time. The same relationship can be used to compensate for the limited bandwidth of the sensors, cables, digitizers or any other measurement equipment used.

3.3.2 Time-of-Flight

The reflections of a transient field in the center of the test volume can be expected after approximately 13-20 ns (time-of-flight to various perturbations of the cell geometry). The polarization of either the electric or magnetic field in the reflected wave is inverted by the reflection (depending on the impedance value of the termination etc.). Multiple reflections appear with an interval time equal to the length of the cell.

Since the excitation from the EMP generator is a single pulse, the reflections will vanish due to small losses inside the cell. No cavity resonances (standing waves) are built up because the losses are not replenished by incoming power as in the CW case.

3.3.3 Higher Frequency Response

When the wavelengths associated with the frequency components of the input pulse are very small compared to the dimensions of the cell, then the front taper of the TEM cell will begin to behave like a horn antenna. These higher frequencies will be radiated from the taper and propagate into the cell in essentially an unguided fashion. Further work is required in order to quantify and detail this phenomenon.

4.0 HIGH-VOLTAGE PULSE GENERATOR

For single pulse excitation, a pulse generator has been integrated into the apex of the TEM cell. This unit is simply a bank of capacitors which are slowly charged then rapidly discharged into the cell. The rise time of the pulse is primarily determined by the inductance of the spark gap switch used to initiate the discharge. The fall time is established by the RC time constant of the cell impedance, R, and the capacitance, C, of the bank.

4.1 Generator Housing

The generator housing, which contains the capacitor, charge resistor and spark gap, normally forms an integral part of the TEM cell, Fig. 22. However, to increase the versatility of the cell, the generator has been designed such that it can be removed and replaced by an adaptor for connection to a low voltage signal source, Fig. 23.

Two aspects of the generator housing geometry are important. The first is the fact that this housing is coaxial in nature and is designed to be compatible with the TEM cell both geometrically and in terms of impedance matching. The inner conductor of the coax is the pulse generator (i.e. capacitors, spark gap etc.) and the outer conductor is formed

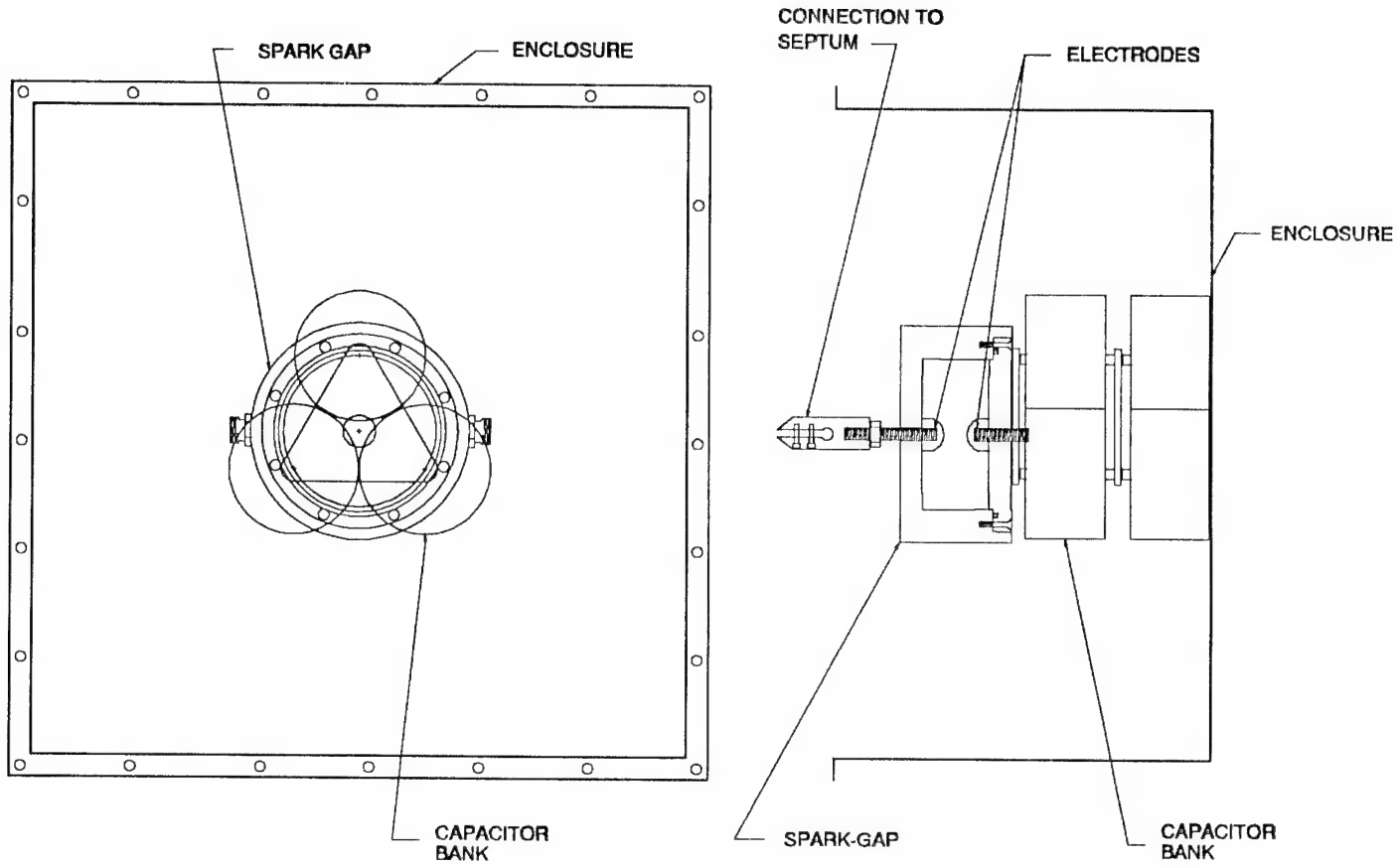

Figure 22: Schematic representation of the EMP pulse generator. The enclosure is 30 cm square to fit on the taper end of the TEM cell. The spark gap and capacitor bank are detailed in Figures. 25 & 26.

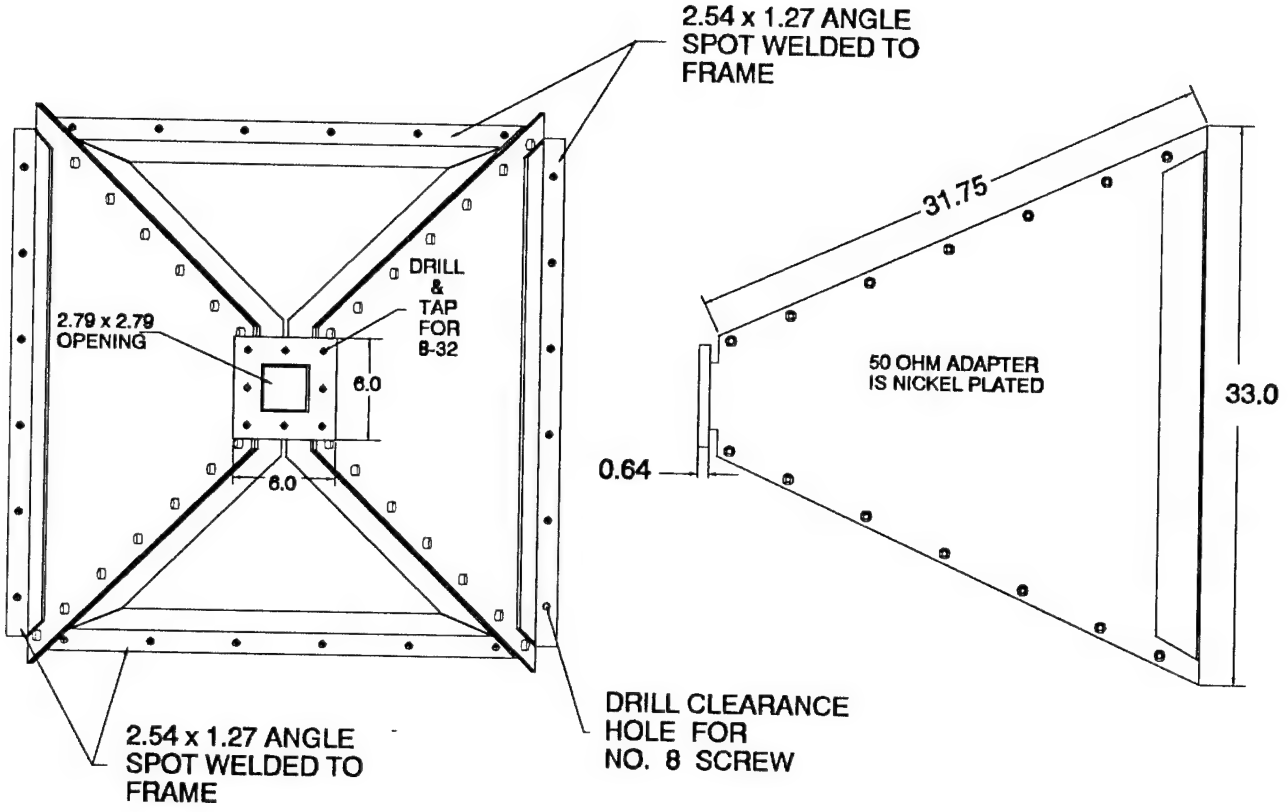

Figure 23: As an alternative to the pulse generator of Fig. 22, an extension to the taper is used to mount a standard N-type co-axial connector to the septum.

by the generator enclosure, Fig. 22. The impedance value for this structure was established by consulting tables for the impedance of a structure with a circular inner conductor and a square outer conductor, Fig. 24. The radius of the inner conductor was estimated from the dimensions and orientation of the charging capacitors, Fig. 25. This is done by equating the area of the triangular capacitor arrangement and the area of a circle with the estimated radius. Once this value and the impedance of the cell (100 Ω) are established, then the dimensions of the outer housing can be determined via Fig. 24. Some compromise in design may be required because the system is required to operate at high voltage and arcing may be a problem.

The second important aspect of the generator housing is the fact that it is at the apex of the input taper and, as such, is the launching point for the fields in the TEM cell. The pulse generator indiscriminately generates many higher order TE_{mn} and TM_{mn}. Ideally some means of eliminating these extraneous modes would exist such that only the fundamental TEM mode would propagate into the cell.

This may be (partially) accomplished by making the generator housing a waveguide with a high cutoff frequency. Since the TE_{mn} and TM_{mn} higher order modes have resonance frequencies below this cutoff value they will be highly attenuated as they propagate along the length of the generator housing. The primary means of increasing the cutoff frequency is to make the spacing between the septum and the walls of the taper as small as possible. At the interface between the cell and the housing, the taper enclosure is 30 cm square which, at $\lambda/2$, corresponds to a frequency f = 500 MHz. This is a factor of six higher than the resonant frequency $f_{R(101)}$ of the first interacting higher-order mode. If the length of the housing is made sufficiently long then the TE_{mn} and TM_{mn} modes will be eliminated and the unit acts as a filter.

4.2 Capacitors

4.2.1 Capacitor Orientation

The capacitors are distributed as indicated in Fig. 25. The excitation should be introduced with the field components in the same orientation they would have when propagating in the cell, but unfortunately this is not possible.

The chosen orientation of the capacitors results in a horizontal electric field and a transverse magnetic field (the electric field which is perpendicular to the proper orientation). This compromise was made because an electric field component in the direction of propagation causes TM modes. These TM modes appear at higher frequencies than the TE modes and, as a result, the bandwidth of the cell is maximized [1].

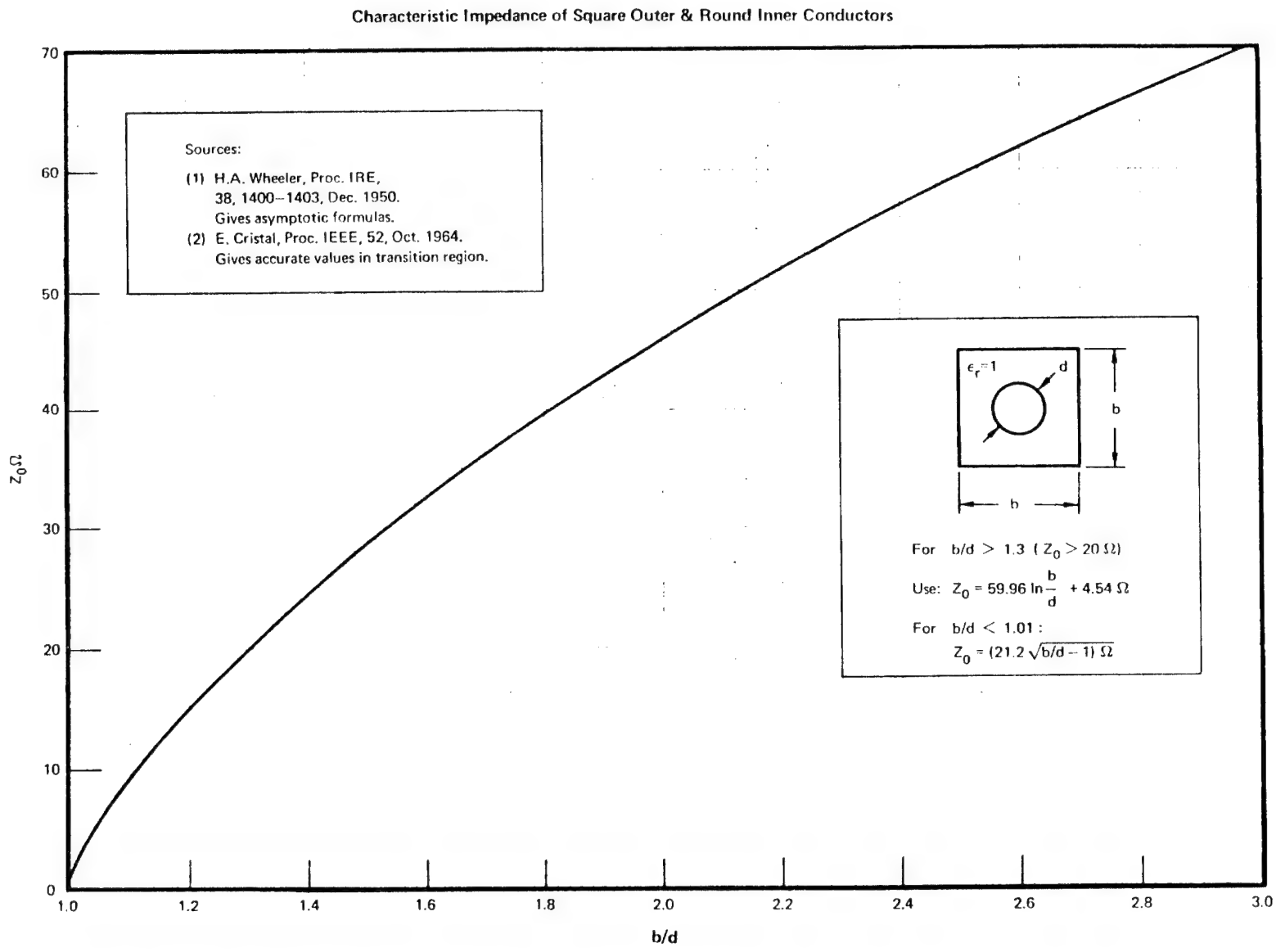

Figure 24: Impedance chart for a square outer conductor with round inner conductor [8].

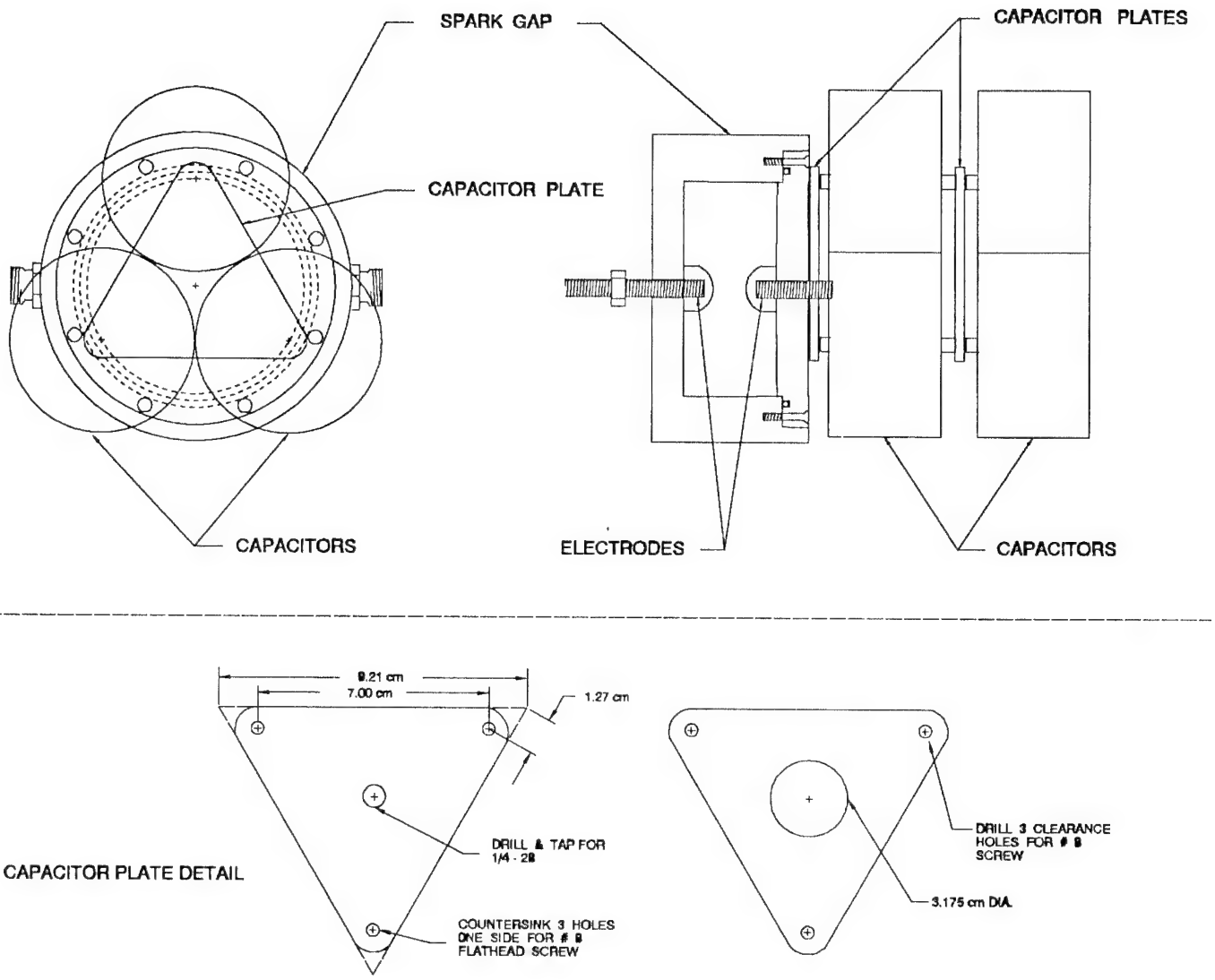

Figure 25: Details of the EMP Pulse generator. The spark gap is further detailed in Fig. 26.

4.2.2 Capacitor Properties

The required half-width time of the field is t_w = 200 ns. The time constant of the discharge circuit should be

$$\tau = RC = t_w / 0.7 = 286\,ns \qquad (11)$$

and with R = Z_o = 100 Ω

$$C = \tau / R = 2.9\,nF \quad . \qquad (12)$$

The high-voltage power supply (HVPS) has a maximum voltage of 75 kV. A low inductance, high-voltage capacitor is needed and many factors must be considered. In this case, properties should include: peak voltage, peak current, wave shape, duty cycle, dissipation factor, power factor, life expectancy, temperature coefficient, etc. Other important characteristics are: the equivalent series resistance, impedance, self-resonant frequency, voltage reversal, dielectric and the dimensions. Detailed discussions on this matter are very complex and beyond the scope of this work. For more information reference [6] should be consulted.

In general, ceramic capacitors have small dimensions, low inductance, low impedance and can handle high voltages. On the other hand they are temperature and voltage dependent. If the temperature of the room is stable and the repetition rate is low, ceramic disc capacitors are a suitable choice. In general, the high voltage types have a lower capacitance and it was necessary to bank the capacitors to achieve the desired values. To lower the inductance, three units were connected in parallel, and two sets were placed in series to ensure that the pulse generator would hold off the required voltage, see Fig. 25. As a result, the capacitance of each unit should be C = 2 x 2.9/3 = 1.9 nF. The generator was designed with a larger value because the capacitance decreases with increasing temperature, voltage and aging. The capacitor type used (Murata Erie, Model DHS60 N4700 202M-40KV) is optimized for linearity with applied voltage. The alternative would have been a unit which is stable in temperature. The former was chosen because it is anticipated that the room temperature will be constant. On the other hand, if the capacitance of the bank changed with applied voltage then the fall time of the pulse would vary as well. Therefore, the pulse shape would not be consistent during testing with varying applied voltages (sub-threat level field testing).

At high frequencies, the pulse impedance of a capacitor appears in series with the load and reduces the voltage across the load. If the pulse impedance is more than 10% of the load impedance, the fast rising portion of the output pulse will begin to roll over before reaching 90% of the peak voltage. A pulse impedance of 5 Ω for large capacitors is not uncommon, but with the bank combination this value is reduced by ⅔. With the high impedance of the cell (100 Ω) the roll-over should not be large.

4.2.3 Interface

The septum/generator interface is shaped according to Fig. 15. Note that the septum has been trimmed such that there is a smooth geometrical transition with dimensions which are small compared to the wavelength used. This has produced a satisfactory result, however, there are a number of other possible configurations which warrant future investigation.

The most promising option is to place excess material on the septum (i.e. more material than is necessary to impedance match the septum) near the interface with the pulse generator. One alternative is to make the septum wider at this point while the other is to increase the height of the septum. The primary contact between the pulse generator and the septum is limited by the spark gap connection and the additional septum material appears to be redundant. However, although the current will primarily enter the cell at the septum contact, it is possible for stray capacitive coupling (from excess septum material directly to the pulse generator) to exist [7]. This will cause an enhancement of the high frequency coupling to the septum. Keeping in mind the discussion of capacitor roll-over (section 4.2.2), this may be a very important compensating element allowing the cell to recover the fast rise time components of the pulse. Unfortunately, implementation of this phenomena is not trivial. The important point to remember is that a pulse generator and field delivery system should be designed simultaneously in order to optimize the resulting electric and magnetic fields.

4.3 Spark Gap

The spark gap is composed of two electrodes in a plexiglass housing which can be filled with a dielectric gas (synthetic air, N_2, SF_6 etc.) with a pressure of up to 80 psig, see Fig. 26. The spacing of the brass electrodes can be varied from 0-2 cm depending on the breakdown voltage required. Since the charge transfer from the capacitors is small, it is anticipated that there will be minimal electrode wear and very little maintenance will be required.

Two factors effect the rise time of the spark gap; the inductance of the spark gap and the resistive phase of the spark:

a) The inductance of the plasma channel is proportional to the length of the spark, therefore the length of this channel must be minimized. This can be accomplished by pressurizing the gap with a highly-insulating gas (i.e. a highly electronegative gas such as SF_6). This works because the breakdown voltage for a gas is determined (to first order) by the product of the electrode spacing and the gas pressure (each gas produces its own breakdown curve and is self-consistent with this pressure-spacing rule). Second order factors include electrode curvature, rate of charge, external ionizing sources (background radiation, etc.), gas contaminants, etc.

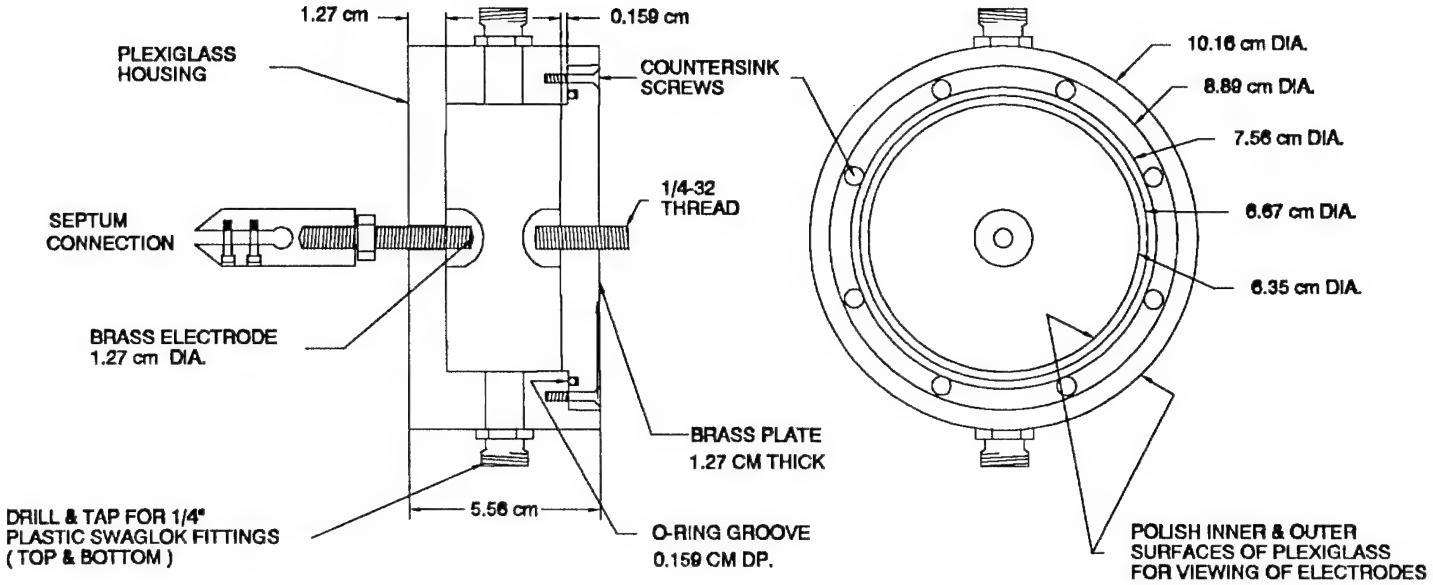

Figure 26: Details of the Spark Gap.

The inductance of the plasma channel can be calculated from [10]

$$L = 2\ell \left[\left(\ln \frac{4\ell}{d} \right) - 1 \right] \text{ nH}, \qquad (13)$$

where ℓ is the length (in cm) and d is the diameter of the spark channel (in cm). Assume ℓ = 1 cm and d = 0.01 cm, then L = 10 nH. With a load impedance of Z_0 = 100 Ω, the time constant τ_L = L/R = 0.1 ns and the corresponding rise time

$$t_L = 2.2\tau_L = 0.22 \text{ ns}. \qquad (14)$$

With ℓ = 1 cm and d = 0.001 cm, L = 14.6 nH and t_L = 0.32 ns.

b) The time constant of the resistive phase can be derived from [7]

$$\tau_R = \frac{88}{Z^{1/3}\, E^{4/3}} \left(\frac{\rho}{\rho_o} \right)^{1/2} \text{ ns} \qquad (15)$$

where E is the field strength in MV/m, and (ρ/ρ_o) is the ratio of the gas density to that of air at STP (standard temperature and pressure).

With 50 kV across 1 cm and a homogeneous field between the electrodes, E is about 5 MV/m. With dry synthetic air in the spark gap the time constant τ_R is 1.3 ns and the corresponding rise time t_R= 2.9 ns. By changing to Sulphur Hexafluoride gas (SF_6), the gap distance ℓ can be made a factor 2.5 smaller, resulting in a field strength of 2.5 x 5 = 12.5 MV/m, a time constant τ_R = 1.0 ns and a rise time t_R = 2.3 ns.

Note that it is important to work with a high field strength, E, in the spark gap. With gas pressurization the gap distance can even be made smaller and thus the field strength, E, larger. The total rise time of the spark is the geometric sum of the two rise times t_L and t_R,

$$t_r = \sqrt{t_L^2 + t_R^2} \qquad (16)$$

which, for air, is t_L = 0.32 ns and t_R = 2.9 ns the total rise time t_r = 2.9 ns.

The rise time of the pulse generator can be calculated in the following manner. The rise time of the spark gap is converted to an equivalent inductance which can then be added, in quadrature, to the geometric inductance of the pulse generator such that

$$L_{eff} = \sqrt{L_{geo}^2 + L_{sg}^2} \qquad (17)$$

The spark gap time constant is given as $\tau_R = L_{sg}/R = t_R/2.2 = 2.9/2.2 = 1.3$ ns. With a load

impedance of R = 100 Ω, then L_{sg} = 1.3 x 100 = 133 nH.

L_{geo} contains the inductance of the capacitor and the connections of the spark gap. Assume L_{geo} is 50 + 50 = 100 nH. The effective inductance is then

$$L_{eff} = \sqrt{100^2 + 133^2} = 166 \text{ nH} \quad . \tag{18}$$

The effective time constant becomes

$$\tau_{eff} = \frac{L_{eff}}{R} = \frac{166}{100} = 1.7 \text{ ns} \tag{19}$$

leading finally to an expected rise time of

$$t_r = 2.2 \times \tau_{eff} = 3.7 \text{ ns} \quad . \tag{20}$$

In this case, it can be concluded that the resistive phase of the spark plays a dominating role in the total rise time. By applying more pressure to the insulating gas in the spark gap, the rise time can be made smaller. With external triggering (eg. laser) the resistive phase can be made shorter and the total rise time even smaller. However, for a rise time t_r = 5 ns, dry synthetic air with a few atmospheres of pressure will be sufficient.

4.4 High-Voltage Power Supply

The high-voltage power supply (HVPS) (Glassman High Voltage, Model PS/ER75R05.0-10) can be adjusted from zero to 75 kV and from zero to 2.5 mA by two 10-turn potentiometers. It is connected to the capacitor via a high-voltage resistor of 100 kΩ which isolates the power supply from the pulse generator. The resistor used is a wire-wound type which ensures high pulse impedance regardless of resistance value. It is also embedded in epoxy and inserted into a teflon tube which is concentrically located in the center of the capacitor bank. This reduces the chance of flash over and simultaneously minimizes the interaction of the charge resistor with the field produced at the launching point.

The time constant of the charging circuit is on the order of 10's of milliseconds which is too small for practical applications. The required charging time of the pulse generator can be altered to approx. 15 seconds by adjusting the current on the HVPS to a very small value. This ensures that there are no misfires when using the TEM cell.

4.5 Triggering

A very simple procedure for triggering the discharge of the capacitor in the transmission line is used;

- The gap distance and the gas pressure are adjusted for the desired charge voltage of the capacitor. To minimize the rise time, a small gap distance and high pressure are required.

- A gap spacing about 10% larger than that required for the desired breakdown voltage of the spark gap (or a higher gas pressure) should be used to ensure that the pulse generator discharges only when desired by the operator. A diagram of the breakdown voltage versus gas pressure at different gap distances can be prepared in advance to facilitate this selection.

- After the capacitors have been charged to the desired voltage, the gas outlet of the spark gap can be opened. The falling pressure caused by the escaping gas initiates the discharge. Once the pulse generator has fired the gap should be repressurized before the HVPS can re-establish the charging voltage. This technique also removes the old gas particles and discharge debris from the spark gap which improves the repeatability of the wave shape. Commercial servo-valves are available which perform this entire function electrically. This allows the firing mechanism to be computer controlled.

This simple triggering method has the advantage of fixing the charging voltage and, therefore, also the field strength. The output voltage of the generator is determined by the pulse impedance of the capacitor and the voltage across the spark gap. The pulse impedance can be a few ohms in series with the load impedance Z_o = 100 Ω, the spark gap has a typical 150 V arc drop. The ratio of the charge voltage and the peak output voltage can be calibrated in advance.

5.0 TERMINATION

The transmission line (input taper - mid section - output taper) is matched to a non-inductive load resistor with value R = Z_o. If well designed, all energy arriving at the end of the transmission line will be absorbed in the termination and no reflections will be observed in the test volume.

The requirements for the non-inductive load resistor can be summarized as follows;

- resistive value 100 Ω, ± 2%;
- temperature coefficient 0.2% per degree C;
- peak voltage 60 kV;

- peak current 1.2 kA;
- peak energy 10 J in 1 μs;
- average power 40 W; and
- duty cycle 1 PPS.

The average voltage and current during 200 ns is about 45 kV and 0.9 kA, resulting in 40.5 MW. Assume about this power should be dissipated in 1 μs and the repetitive rate of the pulse generator is maximum 1 pulse per second, then the average power is about 40 W. A Carborundum ceramic non-inductive resistor, Type 889 AS 500 J was used in the TEM cell.

5.1 Shape

As a result of the relatively large peak voltage (60 kV), the manufacturer's specifications require that the load resistor have a minimum length of about 20-30 cm, depending on the resistor type and the connection method used. This offers the possibility of not only matching the line impedance, Z_o, but also the wave impedance over this length. Fig. 27 is an indication of the panel and overall termination shape which allows the impedance of the line to be gradually matched to the relative resistance value, from 100 Ω to 0 Ω.

The characteristic impedance of a transmission line with a square outer - and a round inner conductor can be calculated from

$$Z_o = 60 \ln \frac{b}{d} + 4.54\ \Omega \qquad \text{for } Z_o > 20\ \Omega,\ \epsilon_r = 1 \qquad (24)$$

where b is the edge of the cross-section of the enclosure and d the diameter of the round inner conductor [8]. Fig. 24 is an indication of Z_o versus b/d and was used to derive the contour of Fig. 27.

5.2 Interface to Septum

Clearly the septum of the TEM cell must be connected to both the pulse generator and the termination. The difficulty with these connections is the fact that both interfaces involve drastic changes in the geometry of the cell and, as such, equally drastic changes in the cell impedance. The empirical design rule used is simply to keep the length of the transition much smaller than the shortest wavelength of interest, the interface can then be treated as a lumped impedance. The capacitive coupling of the septum can then be adjusted (by trimming the septum width, etc.) to minimize reflections.

Figs. 26 & 28 show the details of the interfaces between the pulse generator/septum and termination/septum. The feature of the first is that both the pin and

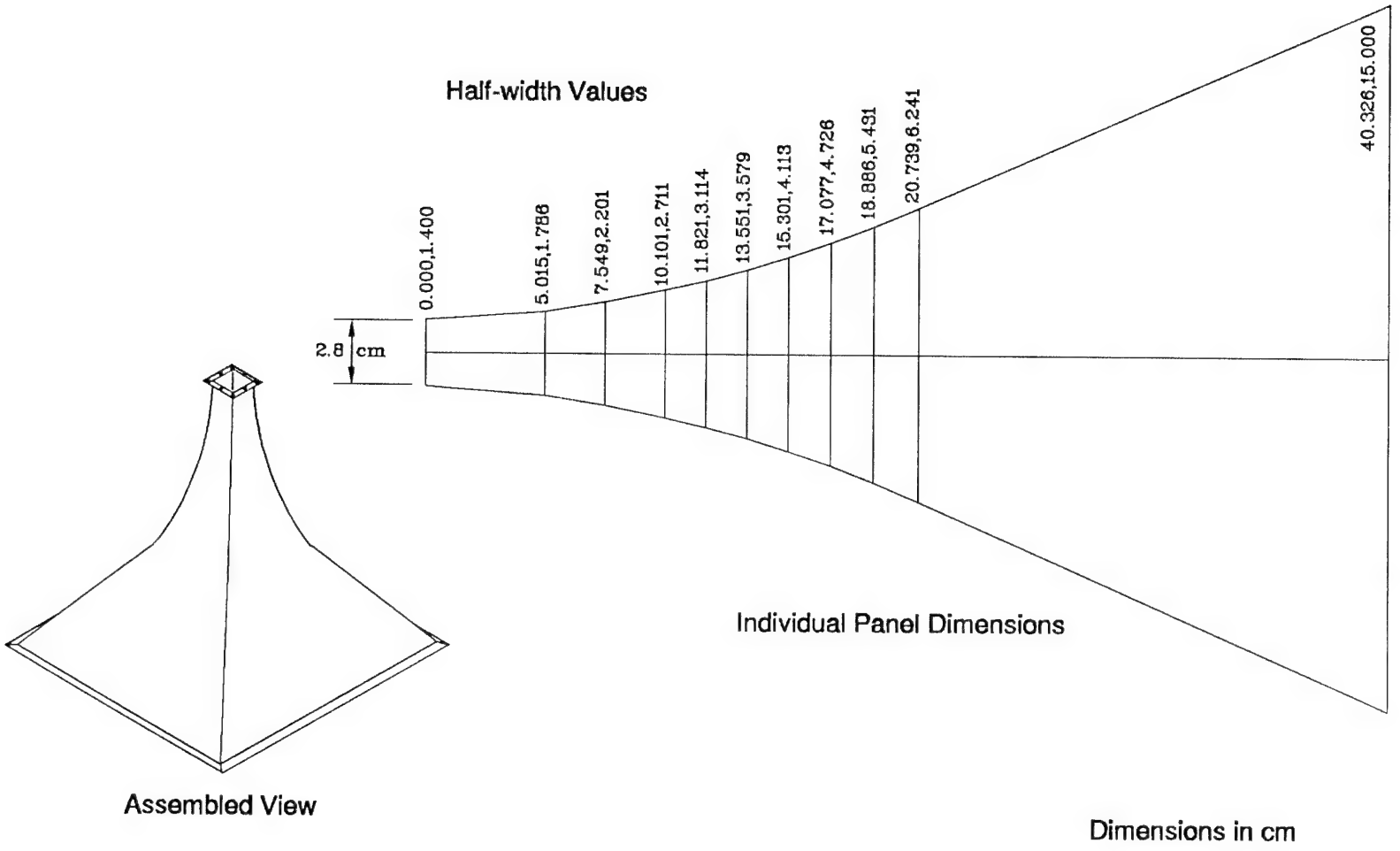

Figure 27: Contour values for the termination outer conductor. The values were determined by varying the geometrical impedance along the length of the terminating resistor from 100 Ω to 0 Ω at the end plate. The dimensions of the panel are determined from Fig. 24 and the technique is further described in the text.

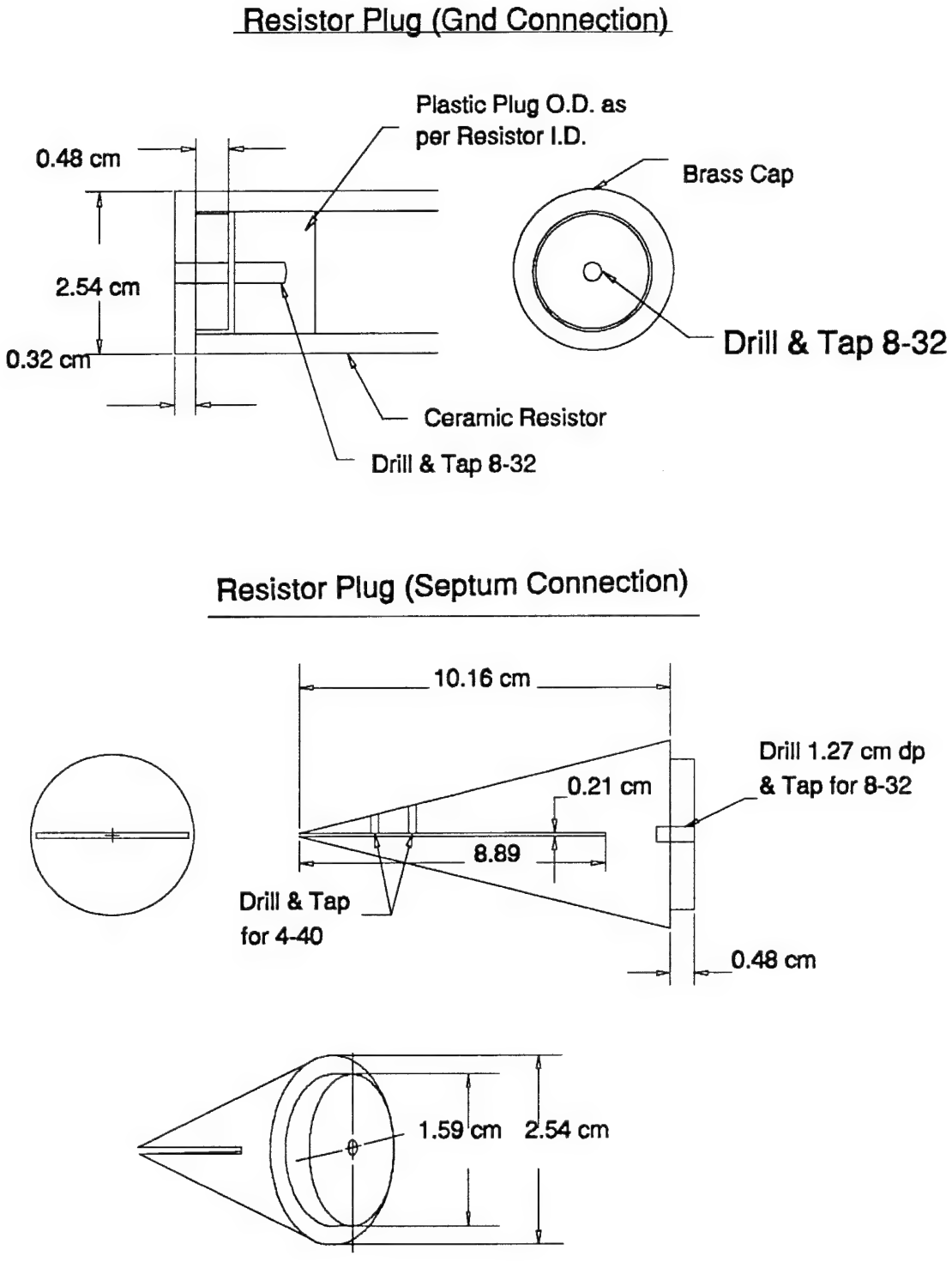

Figure 28: Details of the resistor plugs

the spark gap are tapped with a ¼-20 screw thread which allows the separation between the electrodes to be adjusted without altering the overall dimensions of the pulse generator or septum (note that the nut on the screw thread has been locked in place with a set screw to facilitate this adjustment). The second figure details the transition of the flat septum plate to the circular termination resistor.

6.0 MEASURED FIELDS

Figures 29 and 30 depict the electric and magnetic field waveshapes, respectively, measured at the bottom center of the TEM cell. The E-field measurement is the integrated response (1 μs hardware integrator) of a monopole sensor (EG&G ACD-S3C(R)) and is intended to show the rise time of the pulse. When properly scaled, the peak value corresponds to that anticipated by the 50 kV charging voltage. The 4-4.5 ns rise time value is consistent with the estimated value of 3.7 ns determined in (20).

Figure 30 is the response of a loop probe [9] and depicts the magnetic field waveshape. The time base in this figure has been chosen to show the overall pulse. Although this sensor has a good low frequency response, there is still some sensor droop and the observed pulse width is slightly smaller than both the true value and the predicted value of 286 ns in Eq.(11). Again, when scaled, the peak value corresponds to that expected from a 50 kV charging voltage. Additional details of the complete electrical properties of the cell will be produced in a future publication.

7.0 CONCLUSIONS

In conclusion, implementation of the TEM cell design initially described in DREO Report No. 1084 and further detailed in this report has lead to the development of a means of generating very high-quality pulsed electromagnetic fields for use in both EMP testing (MIL-STD-461C) and R&D activities such as; calibration of sensors, precision measurements, design and testing of transient suppression devices etc.

The electrical parameters of the cell were accurately predicted prior to construction and then achieved through the careful assembly of the cell. A significant effort was made to ensure that the panels described in the various figures of the report accurately reproduce the proper cell dimensions. In addition, the required seams were constructed such that there is negligible perturbation of the current flow. Access to the test volume and sensor mounting plates has been designed to be user-friendly to simplify lengthy test sequences. Design of the high-voltage pulse source and termination of the cell have been carefully optimized and implemented. Finally, the design emphasizes the use of common construction materials and simple assembly techniques for cost reduction.

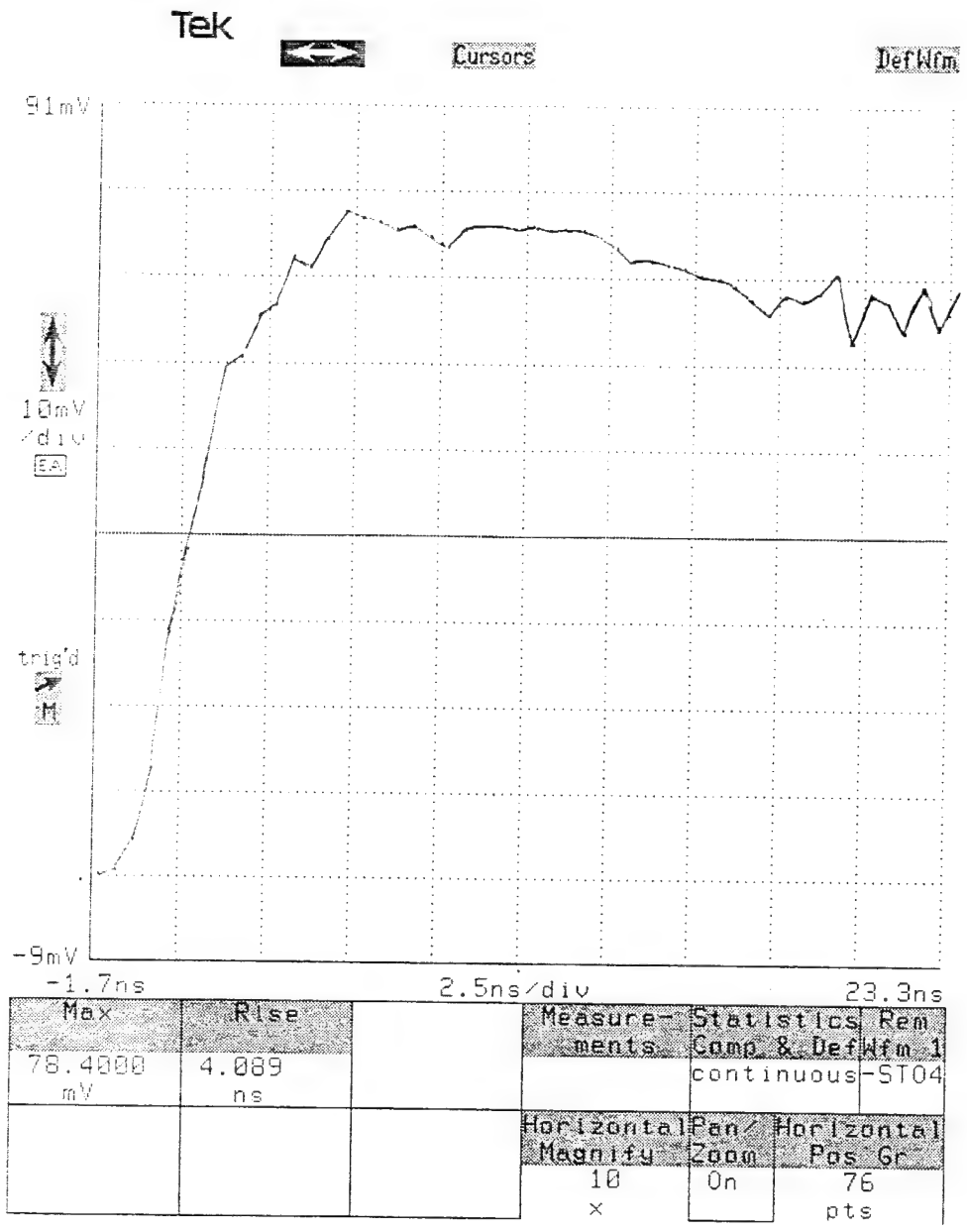

Figure 29: Electric field rise time in the TEM cell. The measurement was made by integrating the response (1μs hardware integrator) of a monopole sensor (EG&G ACD-S3C(R)). When properly scaled, the peak value corresponds to that anticipated by the 50 kV charging voltage.

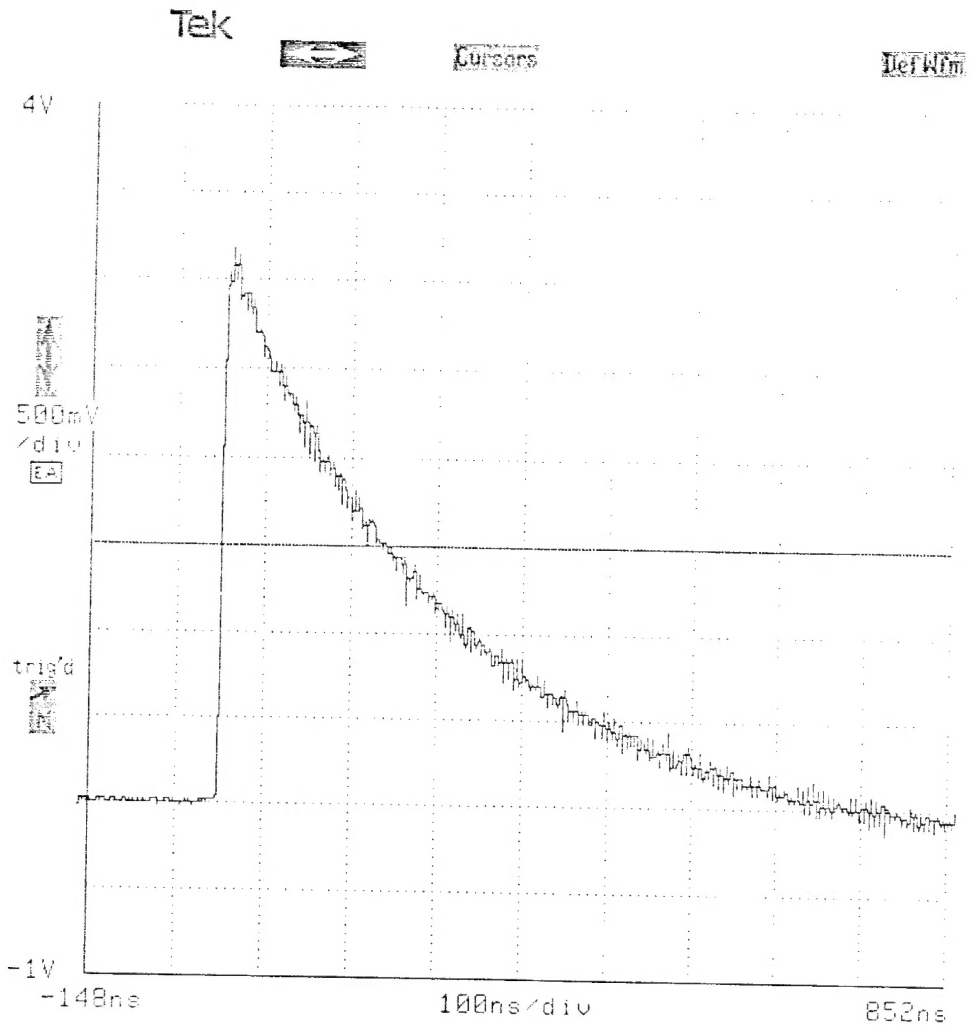

Figure 30: Magnetic field waveshape in the center of the TEM cell. The measurement was made with a loop probe [9]. Although this sensor has a good low frequency response, there is still some droop in the response and the observed pulse width is slightly smaller than the true width. Again, when scaled, the peak value corresponds to that expected from a 50 kV charging voltage.

The result of all this effort is a TEM cell which can produce a pulsed electromagnetic field with a peak value of 50,000 V/m with only insignificant deviations from an ideal double-exponential waveshape. The benefit of having such a accurate and highly reproducible waveform is the simplification in the interpretation of future experimental results.

8.0 ACKNOWLEDGMENTS

The authors wish to thank Peter Sevat for numerous useful discussions and helpful advice over the course of this project. We would also like to thank Paul Deegan of the Communication Research Centre (CRC) model shop whose diligence and attention to detail greatly increased the quality of the mechanical assembly.

9.0 REFERENCES

[1] Sevat, P.A.A., "Design of TEM Cell EMP Simulator", DREO report 1084, June 1991, Ottawa.

[2] Crawford, M.L. Workman, J.L., "Using a TEM Cell for EMC Measurements of Electronic Equipment." NBS Technical Note 1013, Revised July 1981.

[3] Hill, D.A., "Bandwidth Limitations of TEM Cells due to Resonances", J. Microwave Power 18(2):181-195; 1983.

[4] Wilson, P.F., Ma, M.T. "Simple Approximate Expressions for Higher Order Mode Cut-Off and Resonant Frequencies in TEM Cells", IEEE Trans. EMC, EMC-28(3): 125-130; August 1986.

[5] Chen, Y.G., Maxwell Laboratories, Private communication.

[6] Sarjeant, W.J., High Voltage/Pulse Power Technology, Los Alamos Scientific Laboratory Training Course LA-UR-79-1044.

[7] Willis, W.L., High Voltage/Pulse Power Technology, Los Alamos Scientific Laboratory Training Course LA-UR-80-634.

[8] Saad, T.S., Microwave Engineers' Handbook, Volume 1, Artech House, Inc.

[9] Final Draft AEP-21(Edition 1) on NATO Recommended Calibration Procedures for EMP Measurements, NATO Document AC/225(panel VII)D/306

[10] Grover, F.W. Inductance Calculations, D. Van Nostrand Co., 1945.

[11] Dreher, T. Fast Pulse Techniques, E-H Research Laboratories, Oakland Cal.

(highest classification of Title, Abstract, Keywords)

DOCUMENT CONTROL DATA

(Security classification of title, body of abstract and indexing annotation must be entered when overall document is classified)

1. ORIGINATOR (the name and address of the organization preparing the document. Organizations for whom the document was prepared, (e.g. Establishment sponsoring a contractor's report, or tasking agency are entered in section 8.)

Defence Research Establishment Ottawa
3701 Carling Avenue
Ottawa, Ontario, Canada K1A 0Z4

2. SECURITY CLASSIFICATION (overall security classification of the document including special warning terms if applicable)

UNCLASSIFIED

3. TITLE (the complete document title as indicated on the title page. Its classification should be indicated by the appropriate abbreviation (S, C or U in parentheses after the title.)

A TEM Cell for Electromagnetic Pulse Applications: Design Considerations and Mechanical Details (U)

4. AUTHORS (Last name, first name, middle initial)

J.S. Seregelyi, R. Apps, J.A. Walsh

5. DATE OF PUBLICATION (month and year of publication of document)

MAY/95

6a. NO. OF PAGES (total containing information. Include Annexes, Appendicies, etc.)

47

6b. NO. OF REFS (total cited in document)

11

7. DESCRIPTIVE NOTES (the category of the document, e.g. technical report, technical note or memorandum. If appropriate, enter the type of report, e.g. interim, progress, summary, annual or final. Give the inclusive dates when a specific reporting period is covered.)

DREO Report

8. SPONSORING ACTIVITY (the name of the department project office or laboratory sponsoring the research and development. Include the address.)

Defence Research Establishment Ottawa
3701 Carling Avenue
Ottawa, Ontario, Canada K1A 0Z4

9a. PROJECT OR GRANT NO. (if appropriate, the applicable research and development project or grant number under which the document was written. Please specify whether project or grant)

05B01

9b. CONTRACT NO. (if appropriate, the applicable number under which the document was written)

10a. ORIGINATOR'S DOCUMENT NUMBER (the official document number by which the document is identified by the originating activity. This number must be unique to this document.)

DREO REPORT 1263

10b. OTHER DOCUMENT NOS. (Any other numbers which may be assigned this document either by the originator or by the sponsor)

11. DOCUMENT AVAILABILITY (any limitations on futher dissmination of the document, other than those imposed by security classification)

(X) Unlimited distribution
( ) Distribution limited to defence departments and defence contractors; futher distribution only as approved
( ) Distribution limited to defence departments and Canadian defence contractors; futher distribution only as approved
( ) Distribution limited to goverment departments and agencies; futher distribution only as approved
( ) Distribution limited to defence departments; Futher distribution only as approved
( ) Other (please specify):

12. DOCUMENT ANOUNCEMENT (any limitation to the bibliographic announcement of this document. This will normally correspond to the Document Availability (11). However, where further distribution (beyond the audience specified in 11) is possible, a wider announcement audience may be selected.)

13. ABSTRACT (a brief and factual summary of the documents. It may also appear elsewhere in the body of the document itself. It is highly desirable that the abstract of classified documents be unclassified. Each paragraph of the abstract shall begin with an indication of the security classification of the information in the paragraph (unless the document itself is unclassified) represented as (S), (C), or (U). It is not necessary to include here abstracts in both official languages unless the text is bilingual.

This report discusses the mechanical details and some electrical properties of a Transverse Electromagnetic (TEM) cell, an Electromagnetic Pulse (EMP) generator and a terminating network. It is an implementation of a design described in detail in DREO Report No. 1084 (1991) [1]. The cell is primarily designed to generate the fast rise time (few ns) and high field levels (50 kV/m) associated with an EMP. However, it is fabricated in a modular format so that, for example, the high voltage pulse generator can be removed and replaced with an extended taper that will allow conventional EMC measurements to be performed. Such a format significantly increases the versatility of the cell.

14. KEYWORDS, DESCRIPTORS or IDENTIFIERS (technically meaningful terms or short phrases that characterize a document and could be helpful in cataloguing the document. They should be selected so that no security classification is required. Identifiers, such as equipment model designation, trade name, military project code name, geographic location may also be included. If possible keywords should be selected from a published thsaurus. e.g. Thesaurus of Engineering and Scientific Terms (TEST) and that thesaurus -identified. If it is not possible to select indexing terms which are Unclassified, the classification of each should be indicated as with the title.)

TEM Cell
Design
Electromagnetic Pulse
Mechanical Details